Rational Catalyst Design via Imprinted Nanostructured Materials

Mark E. Davis,* Alexander Katz, and Wayez R. Ahmad

Chemical Engineering, California Institute of Technology, Pasadena, California 91125

Received January 10, 1996. Revised Manuscript Received April 8, 1996[⊗]

Progress on the use of imprinting (templating) for the synthesis of nanostructured catalysts is reviewed. In the context of providing a foundation for synthetic mimics, the basic principles of enzyme catalysis are enumerated. With these paradigms in mind, catalytic antibodies, imprinted polymers, imprinted amorphous metal oxides, and zeolites are discussed with respect to their preparation procedures and catalytic properties. These synthetic catalysts are contrasted to one another in order to highlight the advantages and disadvantages of each system. Suggestions for future work on preparing enzyme-mimicking materials by imprinting are provided.

Introduction

Nanostructured solids encompass a broad spectrum of material types whose applications are quite diverse. Areas of science and technology that have significantly benefited from advances in the physicochemical properties of nanostructured materials are mainly those that involve molecular recognition, such as separations, medical diagnostics, drug delivery, sensors, and catalysis. Although molecules and/or materials derived from natural systems, e.g., enzymes for catalysis, antibodies for immunoassays, cyclodextrins for chiral separations, can be utilized for many of the aforementioned functions, there are situations where these entities are unsuitable for application, e.g., harsh environments, regeneration from fouling, etc. Thus, the desire for materials that contain synthetic receptors is high and continues to increase. In this paper, we concentrate on advances in the preparation and physicochemical properties of nanostructured materials for "catalysis by design". Several reviews concerning primarily polymeric materials with imprinted receptor sites for use as separation and drug assay media can be found elsewhere.[1−5]

The lofty goal of catalysis by design has been the dream of many who have worked on abiological as well as biological catalysts. A particularly powerful conceptual approach to abiological catalysis by design has been and continues to be the attempt to translate the principles of enzyme catalysis to nonbiologically derived catalytic materials. It is this line of thought that we illustrate in this review by showing the current progress in fabricating nanostructured materials that attempt to mimic biological, macromolecular catalysts.

Approximately 50 years ago Linus Pauling and colleagues prepared the first nanostructured solids for molecular recognition by molecularly imprinting (or templating) silica gels.[6] Pauling speculated that biological machinery in living systems constructed antibodies by using molecules as imprints or templates.[7] Although this idea is now known to be incorrect, the concept of imprinting to create nanostructured, abiological materials was quickly exploited.[8] Dickey prepared nanostructured silica gels by imprinting the formation of the silica with homologues of methyl orange. Subsequent removal of the imprint molecules yielded gels capable of specific adsorption (see Table 1). Thus, nanostructured solids with specific molecular recognition sites have been reported nearly a half a century ago. It is not obvious to us why these initial encouraging results did not stimulate further work until the 1970s. Although it is clear that these silicas possessed very limited stability,[9,10] the adsorption results are comparable with some of the best data obtained from present-day imprinted materials. Additionally, there was even an early claim of extending this technique to produce silica gels capable of chiral separations.[11] However, it was not until the 1970s that nanostructured materials for molecular recognition surfaced again in the work of Wulff and colleagues who imprinted cross-linked polymers.[1,12] Since the 1970s, and particularly in the 1990s, work on imprinted, nanostructured materials for molecular recognition has burgeoned significantly, particularly in the area of imprinting via noncovalent interactions, to a large extent due to the work of Mosbach and colleagues.[3,4]

Here we provide an overview of imprinted (templated), nanostructured materials for catalytic applications. Enzyme catalysis is briefly introduced to set the

Table 1. Specific Adsorption Results from Dickey[8]

	relative adsorption power[a] for			
silica gel imprinted with	methyl orange	ethyl orange	propyl orange	butyl orange
methyl orange (R = CH_3)[b]	3.5	1.6	1.1	1.1
ethyl orange (R = CH_2CH_3)	2.5	9	2.1	2.2
oropyl orange (R = $CH_2CH_2CH_3$)	2.3	5	20	6
butyl orange (R = $CH_2CH_2CH_2CH_3$)	1.5	2.8	5	15

[a] Relative adsorption power is defined as the ratio of the adsorption power of an imprinted gel to that of a nonimprinted gel. The adsorption power of a gel is the concentration of the adsorbate in the gel divided by the concentration of the adsorbate in the supernatant solution.[8] [b]

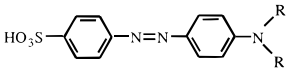

* To whom correspondence should be addressed.

S0897-4756(96)00019-1 CCC: $12.00 © 1996 American Chemical Society

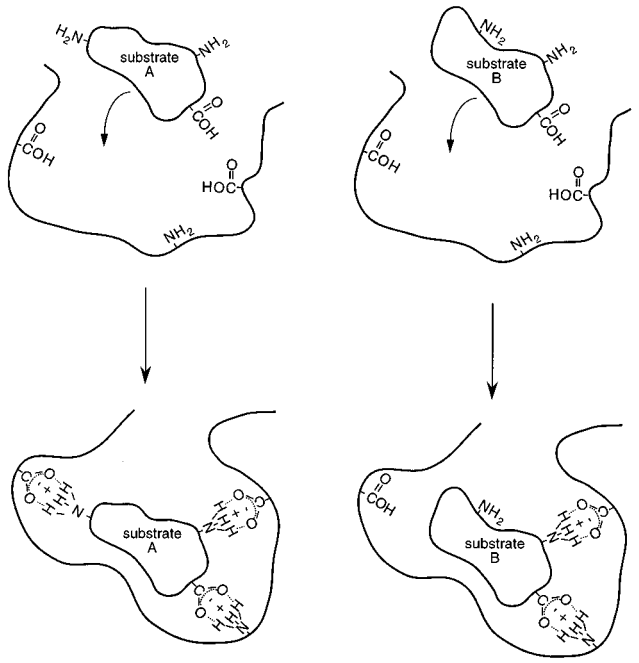

Figure 1. Schematic of the induced fit mechanism for enzyme-mediated catalysis. On the left, substrate A binding induces a change in the enzyme to bring the functional groups into alignment and thus allow catalysis to occur. On the right, the binding of substrate B causes a misalignment of one functional group and catalysis does not proceed (adapted from ref 15).

stage for all the other synthetic mimics. Next, catalytic antibodies are discussed since these macromolecules are catalysts that involve preparation by design and set the benchmarks from which all abiological materials will be compared. Finally, imprinted polymers, amorphous metal oxides and crystalline metal oxides (molecular sieves, zeolites) will be reviewed, and their advantages and disadvantages as designed nanostructured materials for catalysis enumerated.

Enzyme Catalysis: A Model

The elegance of enzyme reactivity is unparalleled in synthetic catalytic materials. Beginning from the time when Emil Fischer proposed his classic lock-and-key theory for enzyme specificity[13] to the now generally accepted induced fit theory of Koshland,[14,15] enzyme catalysis sets the standard to which all other catalytic transformations are compared. To introduce a concept as complex as enzyme catalysis, a brief overview of some of the accepted principles is provided below. A more comprehensive presentation of enzyme structure and function can be found elsewhere.[16]

A limiting-case enzyme model that addresses several important issues related to enzyme catalysis is the induced fit theory of Koshland that is schematically represented in Figure 1. The critical components of this theory are (i) that there is a precise three-dimensional configuration of the amino acid functional groups that must interact with an appropriate reactant (substrate) in order for catalysis to occur, (ii) that the binding (chemisorption) of the reactant produces an appreciable change in the three-dimensional conformation of the amino acids at the active site, and (iii) that the changes in the protein structure produced by substrate binding bring about the proper alignment between protein

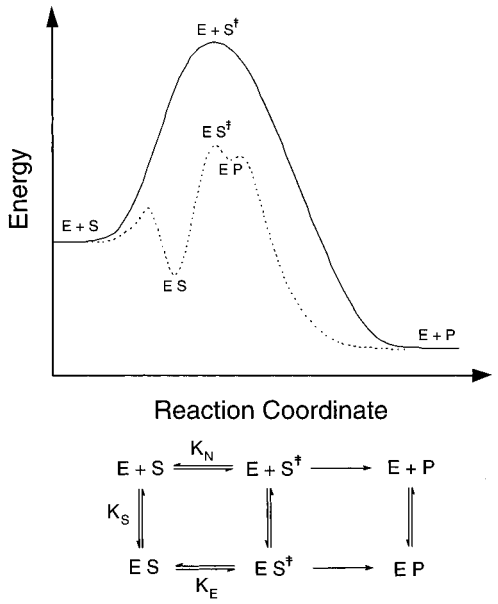

Figure 2. Energy-reaction pathways for hypothetical single-substrate enzymatic and corresponding nonenzymatic reaction.

function groups and the substrate to allow catalytic reactions to occur. A nonsubstrate may still be able to bind but not react due to misalignment of the appropriate interactions. Thus, as Koshland states, the process is not like a "lock-and-key" fit but rather a "hand-in-glove" fit allowing for flexibility.[15] Virtually all enzymes have been shown to have conformational changes upon binding. Gerstein et al. have reviewed the types of movements observed in proteins.[17] They report that nearly all large proteins are built from domains, e.g., β-sheets, α-helixes, etc. Gerstein et al. suggest that when a substrate binds to a particular domain, thermal fluctuations can bring a second domain into contact with the bound substrate, and the newly formed interactions stabilize the "closed" or "bound" conformation.[17] The protein−substrate interactions can be numerous and consist of combinations of interlocking salt bridges, hydrogen bonds and van der Waals interactions that account for the stability and specificity of this state. These domain closures often exclude water from the active site giving rise to a plausible argument for why numerous enzymatic reactions can take place in aqueous media without utilizing water as a nucleophile.[15] In addition to excluding water and providing the proper positioning of catalytic groups, the "closed" state confines substrates and prevents the escape of reaction intermediates. Gerstein et al. conclude that domain closure must be fast, that the energy barrier between the "open" and "closed" states must not be large, that these states are only slightly different in energy, and that they are in dynamic equilibrium.[17] An important feature of this concept is that the alignment of the catalytic and binding groups are optimized for the transition state and that the attainment of this state is energetically unfavorable unless it is supplied with the energy of substrate binding. Figure 2 is a schematic illustration of the energy diagram for a single substrate, enzyme-mediated reaction (enzyme assumed saturated with substrate). Proper substrate binding allows for the bound (closed) state (ES) to be in dynamic equilibrium with free substrate. Upon domain closure, catalytic reaction can occur to transform the bound state (ES) to

an energetically less stable state than the open state of the protein by altering the interactions between the protein and the bound molecule.[17] Note that the upper limit on the rate of catalytic reaction should therefore be fixed by the rate of domain movements. Correlations between the time scales of enzyme movements and catalytic activities have been discussed for enzyme catalysis in low-water environments and show that decreased conformational flexibility yields lower activity.[18] Since the open state is more energetically favored, the product will desorb to return the enzyme to the open state.

As was advanced by Pauling,[19] enzymes accelerate reactions by lowering the activation barrier to the transition state (see Figure 2). How this is accomplished involves a complex sequence of events as illustrated above. Upon initial reflection, it might be expected that evolution has selected to optimize enzymes for their bound (closed) state. However, the induced fit model leads to the conclusion that evolution has selected the protein that optimized both the open and closed states.[15]

Although the aforementioned description of enzymes is simplified for illustrative purposes, some of the essential ideas pertaining to catalysis have been discussed. Thus, it is clear that an extremely complex set of events occur to allow enzyme catalysts to have high activity and selectivity. The question now arises as to how many of the basic principles of enzyme catalysis must be captured in the preparation of synthetic catalysts in order to achieve some form of enzymatic mimicking. Enzymes have been shown to accelerate rates to greater than 10^{17} over background.[20] Weisz has stated that for industrial practice, turnover frequencies of around 1 s^{-1} are sufficient.[21] In numerous cases, enzymatic turnover frequencies are many orders of magnitude higher than the Weisz criterion, e.g., enzymatic turnover frequencies have an upper limit of $\sim 10^7$ s^{-1}. Thus, enzyme mimics may not have to reveal enzymatic rate accelerations in order to be practical catalysts. We believe that the critical feature of enzymatic catalysis that must be preserved is the selectivity at rates around the 1 s^{-1} limit. Additionally, synthetic catalysts must show high product yields and robustness (two features not common in most enzymes) for practical application. This is because it is expected that the cost of a "designed" enzyme-mimicking catalyst would be high and its lifetime productivity must therefore justify its use. With these thoughts in mind, below are illustrated general classes of synthetic catalysts that attempt to mimic features of enzyme catalysis.

Catalytic Antibodies

Pauling first proposed about a half a century ago that a difference between enzymes and antibodies is that enzymes selectively bind transition states of reactions while antibodies bind molecules in their ground state.[22] This paradigm led to the successful construction of catalytic antibodies. Lerner and co-workers[23] and Schultz and colleagues[24] independently demonstrated that antibodies raised (templated) to stable transition-state analogues (TSA) have catalytic activity (see Figure 3). This enormous breakthrough in the rational design of catalytic materials relies on biological machinery for the production of the catalytic antibody. Reviews on the

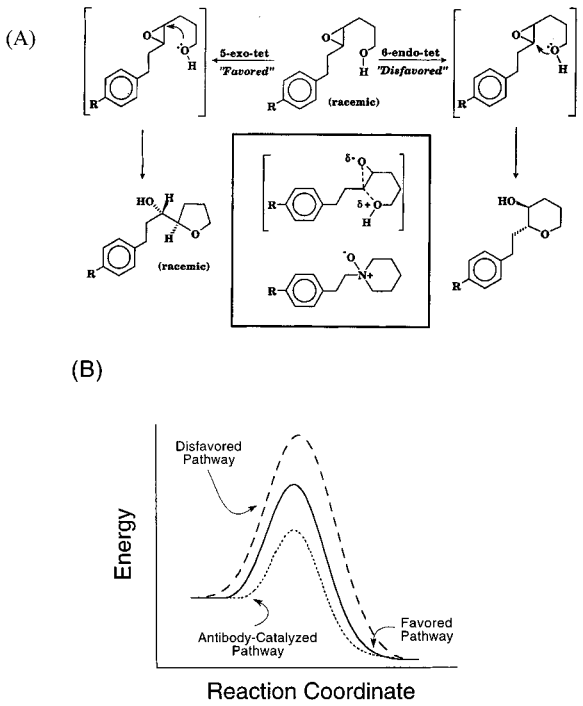

Figure 3. (A) Schematic of a disfavored reaction achieved using a catalytic antibody (pathway ending in the six-membered ring product). Inset: the *N*-oxide TSA (imprint) used to generate the catalytic antibody (bottom) and the proposed intermediate (top). (B) Schematic of energy−reaction pathways for reactions shown in A (adapted from ref 25).

types of reactions catalyzed by catalytic antibodies are available.[25−29] Although catalytic antibodies show higher binding affinities for their transition-state analogues than reaction substrates (implying that they function by stabilizing the reaction transition state), the differences in magnitude in the binding affinities are not sufficient to completely account for the observed rate accelerations.[27] Thus, the question arises of whether the catalytic antibody can in fact catalyze the reaction in a pathway similar to the uncatalyzed or enzyme-catalyzed reactions. Hilvert and co-workers have addressed this issue.[30]

Catalytic antibodies capable of the unimolecular conversion of (−)-chorismate into prephenate with rate accelerations in the range of 10^2-10^4 over the uncatalyzed rate have been prepared using template **1**.[31−33]

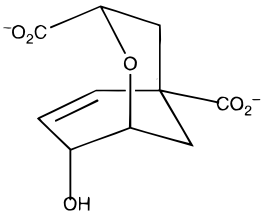

1

This reaction is also catalyzed by the enzyme chorismate mutase with an acceleration of greater than 2×10^6 over the uncatalyzed reaction. Thus, the designed (**1** is prepared to approximate the transition-state of the reaction as shown in Figure 4) catalytic antibody is about 2−4 orders of magnitude less active than the enzyme.[30] Haynes et al. solved the structure of a catalytic antibody with chorismate mutase activity when

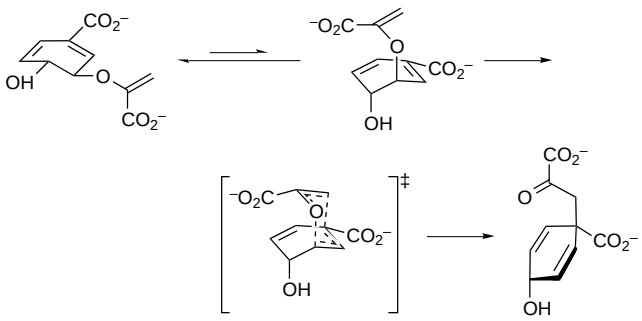

Figure 4. Claisen rearrangement of (−)-chorismate to form prephenate. Reprinted with permission from ref 30. Copyright 1994 American Association for the Advancement of Science.

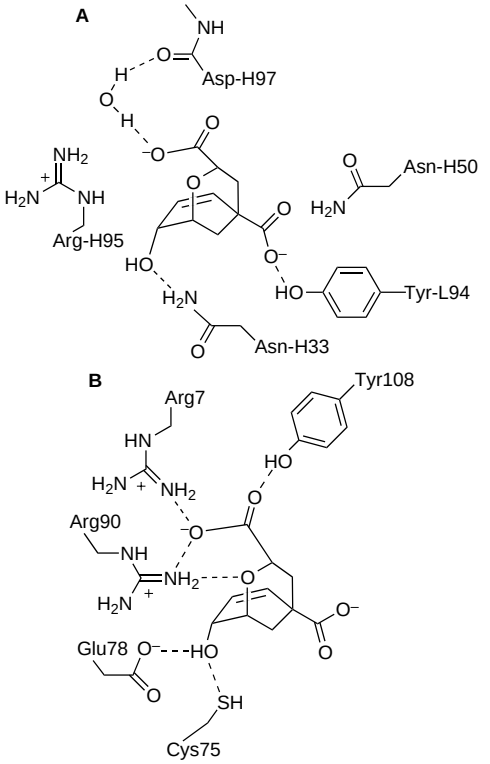

Figure 5. Schematic diagram comparing the hydrogen bonding and electrostatic interactions of the transition-state analogue with relevant side chains in an antibody (A) and enzyme (B). Dashed lines indicate hydrogen bonds. Bonds are not indicated for residues at distances greater than 3.3 Å from the TSA. Reprinted with permission from ref 30. Copyright 1994 American Association for the Advancement of Science.

it was bound with **1**[30] and compared the structure to that of chorismate mutase bound **1**.[34] Schematic representations of the two bound complexes are shown in Figure 5.[30] The structural data reveal that both the enzyme and antibody provide environments complementary to a conformationally restricted transition-state analogue and strongly suggest (by inference) that they both catalyze the isomerization of chorismate by stabilizing the same transition state that occurs in the uncatalyzed reaction.[30] Close inspection of the binding environments reveals combinations of hydrophobic, Coulombic, and hydrogen-bonding interactions, i.e., numerous noncovalent interactions are working in concert. There are 37 van der Waals contacts and three hydrogen bonds between **1** and the antibody,[30] while the enzyme provides a greater number of hydrogen bonding interactions.[34] Haynes et al. speculate that these differences in specific interactions are likely to account for the lower activity of the antibody compared to the enzyme.[30] Thus, this work provides direct evidence that antibody catalysis can be reflected in the design of the transition-state analogue and that it can incorporate some features of enzyme catalysis. As has been cautioned above, there are clear examples where the rate accelerations of catalytic antibodies cannot be completely attributable to templating alone. For example, Thorn et al. catalyzed the base-promoted reaction

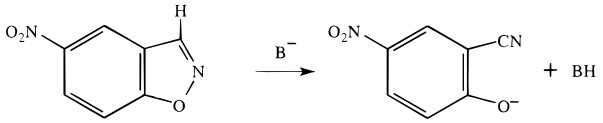

using a catalytic antibody that revealed a rate acceleration of greater than 10^8 over an acetate-promoted reaction rate.[35] However, rate acceleration of this order of magnitude can be achieved by conducting the acetate-promoted reaction in dry acetonitrile rather than water.[36] Thus, Thorn et al. were not able to separate the effects of individual factors such as the apolar nature of the antibody active-site region (partitioning of substrate from aqueous media to "dry" active site; solvation of carboxylate active site more like dry acetonitrile than water) and the proper alignment of active site base (templating).[35]

The work of Hilvert and colleagues clearly demonstrates that the concepts currently employed in the preparation of catalytic antibodies can be successful in allowing the rational design of catalytic materials that do not appear to function too differently than enzymes. However, Stewart and Benkovic have recently placed limits on the expected behavior of catalytic antibodies.[37] First, Stewart and Benkovic state that the affinity of enzymes can reach values of 10^{-24} M, while the best antibodies give 10^{-9} M. This difference in binding suggests that significant progress in the design of catalytic antibodies needs to be made for their rate accelerations to match those of enzymes. However, as previously mentioned, this may not be necessary for the practical application of catalytic antibodies. Second, antibodies are elicited to a single specific structure while enzymes have evolved to bind a series of structures along the reaction pathway[37] (see previous discussion on open and closed states of enzymes and their evolution). Therefore, the structural dynamics of antibodies are not optimized for catalysis as are those of enzymes. These conclusions are intuitively obvious by considering biological applications of antibodies and enzymes.

The ultimate goal of the rational design of catalytic materials involves two principles: (i) that the atomic structure−reaction property relationships are known and (ii) that synthetic methodologies to create defined atomic arrangements are available. For catalytic antibodies, point ii is possible via the use of biological machinery. For point i, the structure−property relationships are not known but induced by the use of a transition-state analogue (TSA) as imprint. The degree to which the TSA actually approximates the true transition state can have a large effect on the magnitude of the rate acceleration.[16] Also, dissimilarity of the TSA to the product is useful in minimizing product inhibition,[35] which may be particularly important for reactions that are not strongly exothermic, as discussed in the next section. In our opinion, catalytic antibodies are

good demonstrations of the rational design of catalysts. Catalytic antibodies can be prepared to catalyze disfavored reactions[29] (see Figure 3) and reactions that cannot be accomplished by enzymes (over 60 different reactions have been catalyzed by antibodies including chiral conversions: see ref 37 and references therein).

There is little doubt that catalytic antibodies will find applications in niche areas of fine chemical syntheses and medical diagnoses. Several factors currently limit their use in other sectors of catalytic technology. For example, and as with enzymes, catalytic antibodies are not able to function in harsh physical, e.g., high temperature, or chemical, e.g., high- or low-pH environments. Also, to our knowledge, no report on the long-term stability of catalytic antibodies has appeared. Other issues such as the lifetime productivity (nonmillimolar product concentrations; gram-scale preparations of single enantiomers have now been reported[38]), the cost, and the sophistication and scale of antibody synthesis all currently limit their applicability for use in large-scale chemical synthesis. Despite these shortcomings, the invention of catalytic antibodies is a revolution in rational catalyst design. We note that from a practical standpoint, rational catalyst design must compete with combinatorial synthesis/selection methods for application. (The preparation of catalytic antibodies employs a rational design of the TSA and a selection method for obtaining the antibody.) For biologically based synthetic methods/catalysts, it appears that combinatorial technologies show many advantages over pure, rational catalyst design in ultimately achieving the objective of preparing a catalyst for a particular reaction. However, for abiologically based preparations/catalysts, combinatorial methods have thus far not revealed the same types of successes as shown in biological systems. Therefore, the question of postsynthetic selection (combinatorial methods) versus presynthetic selection (design) is a question that will continually be asked and whose answer will continually change. Next, we discuss nanostructured abiological materials whose preparations have in many respects borrowed concepts from the field of catalytic antibodies in order to attempt to achieve the rational design of catalytic materials that overcome the aforementioned disadvantages of catalytic antibodies.

Imprinted Polymers

The imprinting of organic polymers represents a general strategy to endow randomly oriented, carbonaceous materials with a "memory" for a particular molecule. This "memory" is created by positioning functional groups of the polymer into a specific geometric arrangement that affords binding interactions between the polymer and the imprint. This procedure is similar in principle to the early work of Dickey on imprinting silicas.[8,9] However, the advantage of polymeric systems is that functional groups other than hydroxyl groups (the only functional group in silica) are available to provide interactions with the imprint. When imprinting polymers, several synthetic methods have been developed[1,4,39] and new ones are continually being reported[40] to design the positioning of the polymer functional groups for optimum imprinting efficiency. Early work in this area employed covalent rebinding interactions between the polymer framework and the adsorbing molecule.[1] That is to say, a side chain on the imprint was prepared such that it could be incorporated into the polymer backbone. More recently, noncovalent interactions, which are the method of choice in natural systems such as antibodies and enzymes, have generally gained preference for the synthesis of imprinted solids because of the relative ease of preparation.[4,41] It is noteworthy that hydrogen-bonding interactions have become particularly important in noncovalent polymer imprinting due to the specific geometric directionality associated with such bonds.[42] Because the molecular recognition characteristics of imprinted polymers are a direct consequence of their rigidly cross-linked surface structure,[1] applications of the imprinting method rely on the "lock-and-key" principle.[13] These applications include catalysis, which is accomplished by imprinting the polymer with a TSA in a fashion similar to that described for antibody catalysis. The critical component in optimizing imprinted polymers for a particular application is the design of the binding interactions between the imprint molecule and the polymer functional groups.

Imprinted polymers are typically copolymers prepared from two or more monomers. One of the monomers is used to create the inert "scaffolding" that provides mechanical support for the imprinted, nanoporous structure. The selection of these monomers is based on the ability to achieve high cross-link densities. An example of such a monomer is ethylene glycol dimethacrylate **2**. A second monomer is used in an imprinted

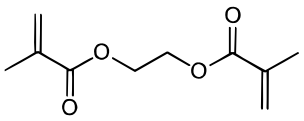

2

polymer as the binding monomer and is selected based on its ability to form favorable binding interactions to the imprint molecule. Examples of binding monomers that have been used include methacrylic acid **3** for base-containing imprints and 4-vinylpyridine **4** for acid-containing imprints.

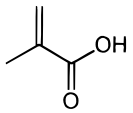

3

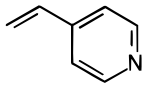

4

The binding monomer forms the interface between the bulk inert monomer and the imprint molecule as illustrated in Figure 6. A compilation of the different monomers that have been used in imprinted polymer syntheses can be found elsewhere.[4]

Two general methods of regulating the molecular-level positioning of the binding monomer have been reported for imprinted polymers utilizing noncovalent rebinding interactions: the controlled distance method and the self-assembly method. The controlled distance method places the binding monomer in a predetermined geometric position relative to the imprint molecule and usually involves the synthesis of a molecule that is a composite of the imprint molecule and the binding

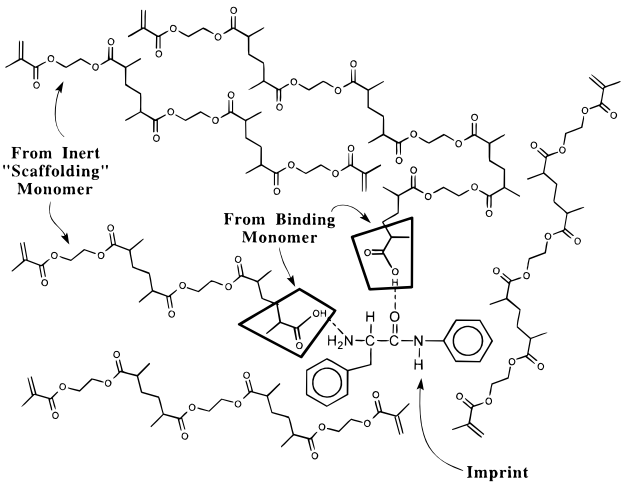

Figure 6. Schematic diagram showing the configuration of inert "scaffolding" monomer, binding monomer, and imprint in a typical imprinted polymer (adapted from ref 43).

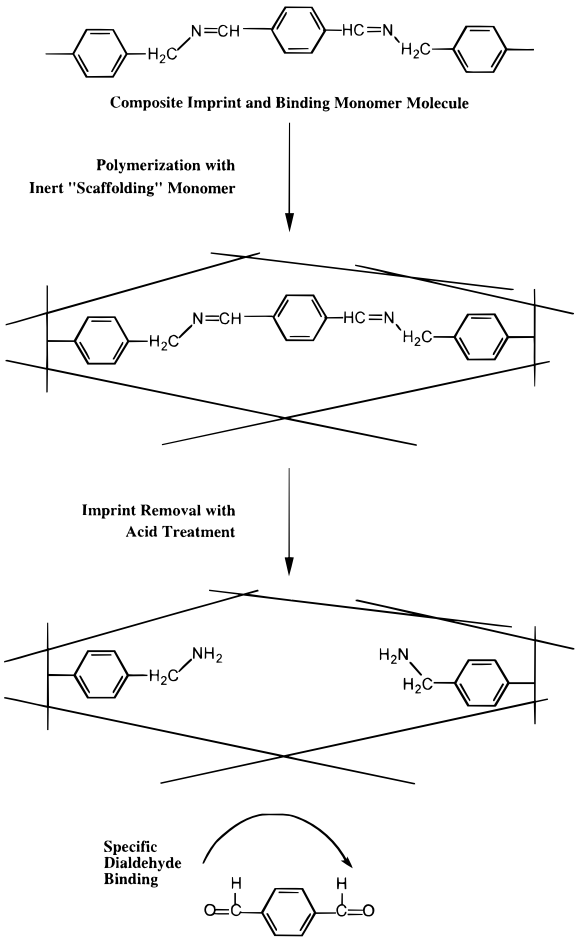

Figure 7. Example of an imprinted polymer preparation for the binding of a dialdehyde using the controlled distance method (adapted from ref 46).

monomer linked by covalent bonds.[40,44−46] Removal of the imprint by chemical reaction from the imprinted polymer leaves the residuals of the binding monomers in positions determined by the imprint molecule. The resulting nanopore has binding monomers situated in predetermined conformations and distances from one another. An example of this type of preparation is illustrated in Figure 7. An advantage of this method includes limited binding to the imprint molecule by the solvent (and other nonspecific binding molecules) in the monomer solution prior to polymerization. This advantage is manifested in the fact that imprinted polymers synthesized by the controlled distance method show only a very weak selectivity dependence on the solvent that is used in the polymerization.[1] This is in contrast to polymers synthesized by the self-assembly method (vide infra). However, considering the extremely sharp distance dependence of hydrogen-bonding and van der Waals interactions,[47] it is not at all obvious that the controlled distance method affords any practical advantages in bringing about optimum binding configurations for maximum interaction between the binding monomer and the imprint over the self-assembly method.

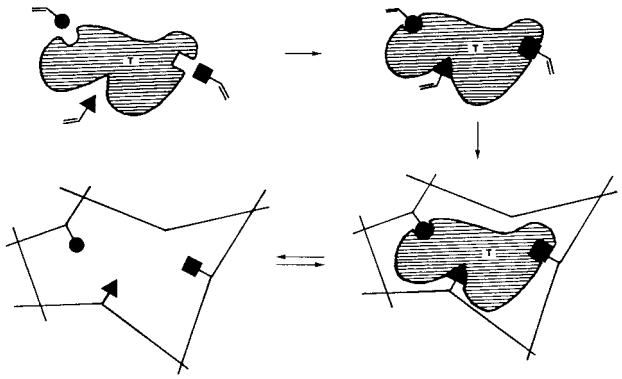

Figure 8. Schematic representation of the self-assembly method in polymer imprinting. Reprinted with permission from ref 1.

The self-assembly method of imprinted polymer formation is schematically represented in Figure 8.[3,4,41] With this method, the binding monomer and imprint molecule are allowed to self assemble in the prepolymerization mixture in a way that maximizes the binding interactions between the two species. After polymerization, the imprint is extracted from the polymerized material, leaving a nanopore that is supposedly selective to the binding of the imprint molecule (due to the complementary positioning of the binding monomers). The self-assembly method suffers from a severe dependence on the specifics of the polymerization conditions such as the particular solvent and temperature.[43,48,49] Since no systematic comparisons of the controlled distance and self-assembly methods for noncovalent polymer imprinting have been reported to date, it is unclear at this time whether one method is really superior to the other.

The potential advantages of imprinted polymers over catalytic antibodies for practical applications are straightforward to envision. Imprinted polymers are relatively simple to prepare and can be formed rapidly (2−3 days) in large scale. They also show good mechanical, chemical, and thermal stability, due to their highly crosslinked nature. Additionally, imprinted polymers can be reused over 100 times and stored in the dry state at ambient temperatures for several years without loss of recognition capabilities.[41] In addition, the potential to reuse the polymers time and time again without loss of molecular recognition capability may be of value.[41]

Despite the apparent advantages of imprinted polymers over biologically produced materials, significant work remains before imprinted polymers approach the selectivity and catalytic efficiency of their antibody counterparts. This is illustrated below. Imprinted polymers have been prepared for use as chiral separa-

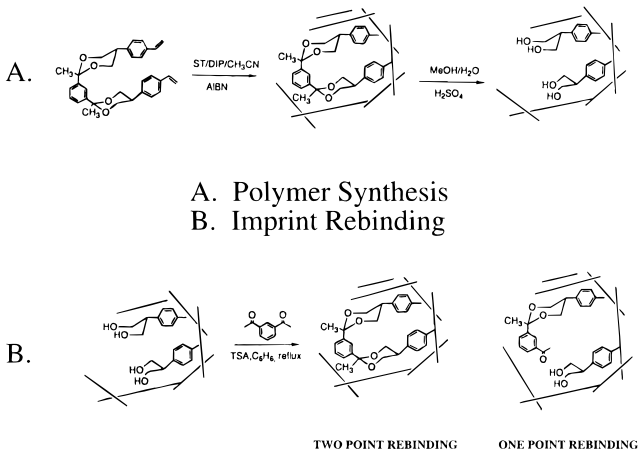

Figure 9. (a) Preparation of imprinted polymer by Shea and Sasaski for covalent binding of diketone and (b) binding of a diketone in imprinted nanopore yielding both one point and two point rebinding (adapted from ref 51).

tion media, and this area has been reviewed elsewhere.[4] Most enantiomeric separations have selectivities less than 10 with imprinted polymers. This represents an approximate binding energy difference of 1.4 kcal/mol at room temperature, which is significantly less than the average energy of a single hydrogen bond.[42] This apparent paradox can be explained by the fact that imprinted polymers are comprised of a few selective sites (that can sometimes rival the molecular recognition capabilities of antibodies[50]), and a vast majority of relatively nonselective sites. The site heterogeneity present in an imprinted polymer has been investigated by FTIR and ^{13}C CP/MAS NMR experiments.[51] Dynamic binding experiments were performed on an imprinted polymer that covalently bound a diketone molecule to the polymer with the release of up to two water molecules (shown in Figure 9). Results from this investigation suggest that nanopores in the imprinted polymer consist of a combination of one-point and two-point binding sites. Upon rebinding the diketone to the polymer with initially vacant nanopores (shown in Figure 9b), the percentage of overall binding sites occupied that were two-point binding sites continuously decreased with binding time, exemplifying the heterogeneous nature of the imprinted polymer surface. Note that some of the nanopores that comprised one point binding sites could be converted to two point binding sites by performing a Soxhlet extraction of water immediately following rebinding.[51] This result suggests that the water molecule released during the binding of the first ketone group of the imprint molecule may noncovalently bind to the second ketone group of the imprint molecule and thereby impede the covalent binding of the second ketone group to the polymer framework in the same nanopore. It is apparent, however, that factors other than water contamination may be responsible for the existence of the one point binding sites observed in this particular system, since the imprinted polymer still possessed both one- and two-point binding sites even after the water extraction procedure. A further manifestation of the existence of heterogeneous binding sites can be found in the work of Sellergren and colleagues on noncovalently imprinted polymers.[43,48,49,52] This group investigated polymers that were imprinted with amino acid amide derivatives

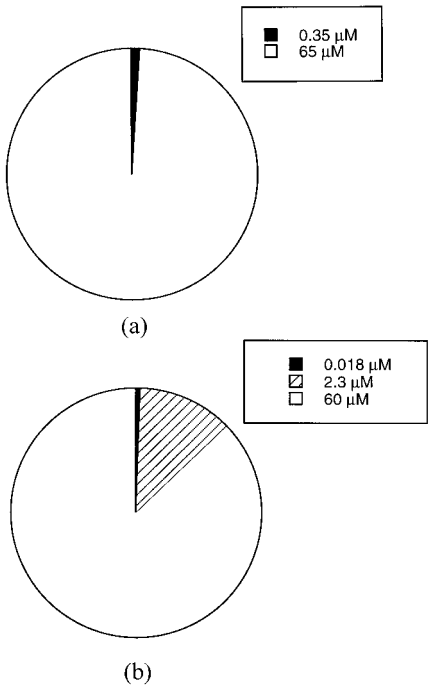

Figure 10. Fraction of binding sites found in (a) theophylline imprinted polymer and (b) diazepam imprinted polymer. Data taken from ref 55.

using both equilibrium batch and kinetic chromatographic binding experiments. These two methods consistently gave the same picture of the imprinted polymer surface as one that contains very few selective sites and a vast majority of nonselective sites. Typical values for the percentage of sites that were found to be nonselective are on the order of 99.8% of the total number of possible binding sites based on the amount of imprint originally extracted from the polymer.[48] The heterogeneous nature of the binding sites in imprinted polymers highlights the cause of the main limitation of imprinted polymers for molecular recognition: few selective sites are available for binding and catalysis with the majority of the binding sites offering relatively poor selectivity. The existence of nonselective sites is a fundamental difference between imprinted polymers and enzymes and antibodies.[53]

Comparisons of the binding specificity found in antibodies and imprinted polymers have been reviewed elsewhere.[54] Vlatakis et al. investigated the binding of the drugs theophylline and diazepam on imprinted polymers synthesized by the self-assembly method.[55] Both the theophylline and diazepam imprinted polymers performed favorably in their selective rebinding of the imprint drug over various other compounds and in some cases revealed higher selectivities than natural antibodies. However, the inherent heterogeneous nature of the imprinted polymer surface was apparent in this study by the fact that a three-site binding model was necessary to numerically fit the experimentally measured adsorption isotherm for the case of diazepam (a two-site binding model was necessary for theophylline). Furthermore, the most selective sites on the diazepam imprinted polymer, which had binding constants in the nanomolar regime, comprised only 0.45% of the total binding sites, while the remaining sites had binding constants in the micromolar regime. These results are graphically summarized in Figure 10 for the diazepam

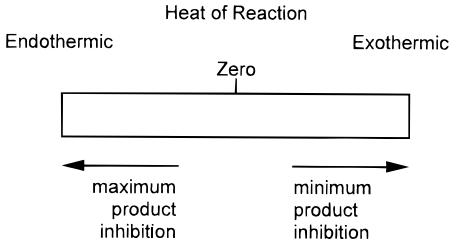

Figure 11. Schematic representation of the relationship between enthalpy of reaction and the degree of product inhibition expected for a rigid catalyst such as an imprinted polymer (or imprinted silica).

and theophylline imprinted polymers. Other investigations comparing imprinted polymer performance to antibodies have been completed with similar results concerning the heterogeneous population of sites in the polymer.[50] The main limitation of the imprinted polymers in these investigations is that the sites have varying degrees of affinity for the imprint molecule. We note that no known studies have yet been performed that compare the relative magnitude of the binding constant of an antibody to that obtained with an imprinted polymer for the same compound and under the same conditions.

Imprinted polymers have been used to catalyze various organic chemical reactions. The strategy used with imprinted polymer catalysts is to stabilize the transition state for a particular reaction, thus lowering the activation energy barrier for reaching the transition state and thereby increasing the rate of reaction.[56,57] Therefore, the use of a TSA imprint is employed in analogy to catalytic antibodies. Of importance to understanding the reactivity is the fact that the TSA molecules are rigidly held in a particular conformation in the polymer and that the lack of conformational flexibility of the polymer does not allow for an "induced fit" as with enzyme catalysis. Thus, product inhibition can be a significant problem in the catalytic applications of imprinted polymers (and imprinted amorphous metal oxides, which are discussed in the next section). If the product is structurally too similar to the transition state that is being stabilized by the imprinted material, it will be difficult to desorb it from the polymer framework once turnover has been achieved. It would be useful to be able to predict a priori the reactions that are most likely to proceed on an imprinted polymer catalyst. We believe that the Hammond postulate most likely can provide some useful information in this regard. This postulate states that for an exothermic reaction, the transition state resembles the reactants and for an endothermic process the products.[58] It is therefore conceivable that exothermic reactions will avoid product inhibition to a greater degree than endothermic ones, with the degree of exothermicity representing the degree to which product inhibition is avoided as schematically represented in Figure 11. It is anticipated that this will be true of catalytic antibody systems[35] and especially true of rigid catalytic systems such as imprinted polymers and silicas, which are highly cross-linked. Reactions performed with imprinted polymer catalysts are given in Tables 2 and 3, and in Table 3 our calculated standard enthalpies of reaction for selected reactions conducted on imprinted solids and antibodies using ab initio methods[59] are presented. Most of the reactions

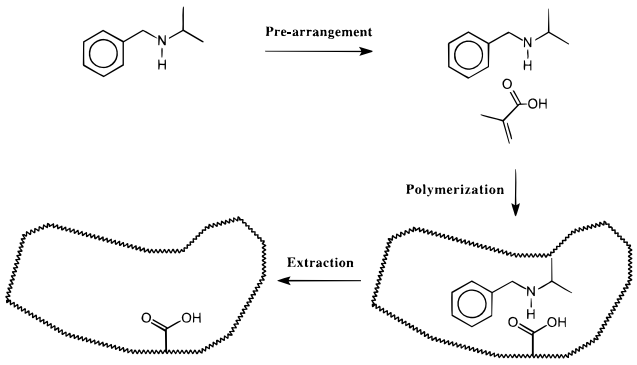

Figure 12. Polymer imprinting scheme used by Müller et al. for the deydrofluorination reaction (adapted from ref 69).

Table 2. Reactions on Imprinted Polymers

no.	reaction	ref
1	α-proton exchange of phenylalaninanalide	66
2	photodimerization of *trans*-cinnamic acid	72
3	stereoselective synthesis of threonine and allothreonine	73
4	stereoselective synthesis of *trans*-1,2-cyclopropanedicarboxylic acid	77
5	hydrolysis of adenosine triphosphate	78

performed on imprinted polymers, antibodies, and imprinted silicas that are listed in Table 3 are indeed exothermic, including those that are difficult to accomplish by alternative techniques.[60,61]

A general history of catalysis with imprinted polymers can be found elsewhere.[1−3,39] Here, we discuss a few specific examples to illustrate points of concern when using imprinted polymer catalysts. The esterolysis of *p*-nitrophenyl acetate (reaction F in Table 3 and below) by imprinted polymer catalysts has been investigated by several research groups:[62−65]

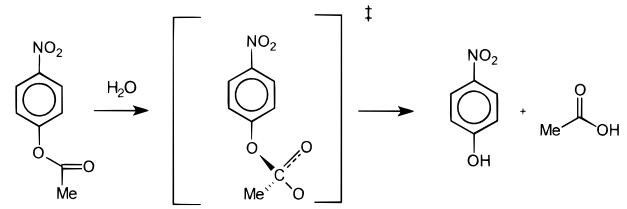

Robinson and Mosbach used the organophosphorous TSA **5** to imprint the polymer.[63] This imprint is used

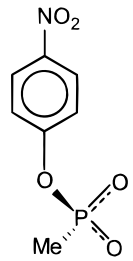

5

to mimic the transition-state geometry of the reactant carbonyl carbon by providing a tetrahedral arrangement within the TSA by the use of phosphorus. The catalytic results from this imprinted polymer show only a mild rate enhancement that is approximately a factor of 1.6 larger than a nonimprinted reference polymer for 10% methanol in water (pH 8.0).[63] Ohkubo et al. used ab

Table 3. Standard Heats of Reaction for Selected Antibody, Imprinted Polymer, and Imprinted Silica-Catalyzed Reactions

no.	reaction	catalyst	ΔH (kcal/mol)	kinetic information[a]	ref
A	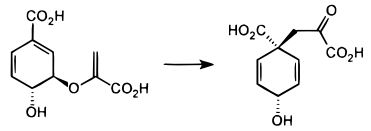	antibody	-12.9	$k_{cat}/k_{uncat} > 2.0\times10^6$	31-33
B	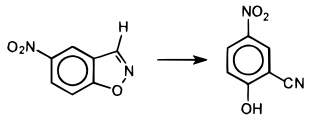	antibody	-51.99	$k_{cat}/k_{uncat} = 2.1\times10^4$	35
C	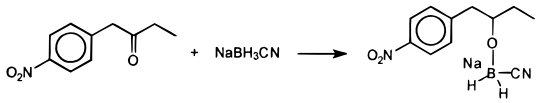	antibody	-34.57	$k_{cat}/k_{uncat} = 1.7\times10^6$	61
D	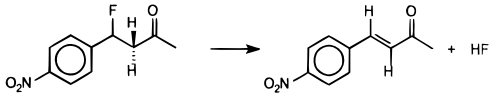	antibody and polymer	-3.67	$k_{cat}/k_{uncat} = 1.5\times10^3$ (AB)[b] $k_{cat}/k_{uncat} = 7.5$ (P) TOF= 14/day (P)	69-71
E	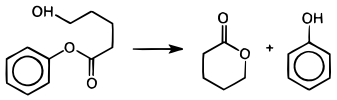	antibody[c] and silica	-1.78	$k_{cat}/k_{uncat} = 167$ (AB) not reported for silica	92, 93
F	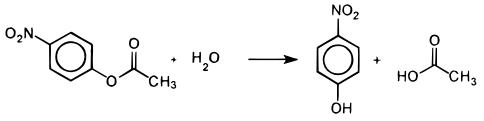	polymer	-5.83	$k_{cat}/k_{uncat} = 6.7$	62-65
G	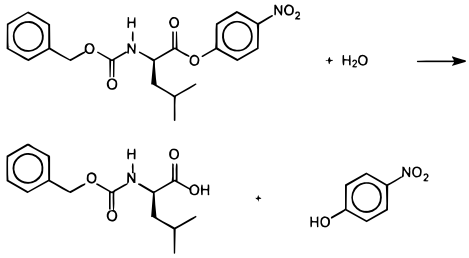	polymer	-15.69	$k_{cat}/k_{uncat} = 3.7$	68
H	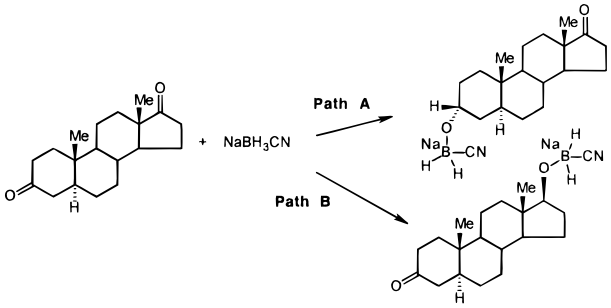	polymer	-29.52 (Path A) -27.09 (Path B)	not reported	74
I	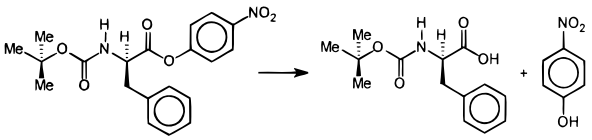	polymer	-84.39	k_{cat}/k_{hom}[d] = 10	75
J	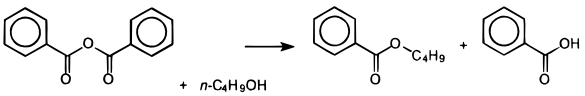	silica	-4.84	not reported	81
K	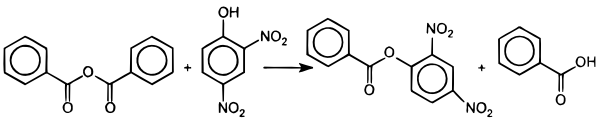	silica	+10.84	$k_{cat}/k_{uncat} = 33.4$	83, 85

Table 3 (Continued)

no.	reaction	catalyst	ΔH (kcal/mol)	kinetic information[a]	ref
L	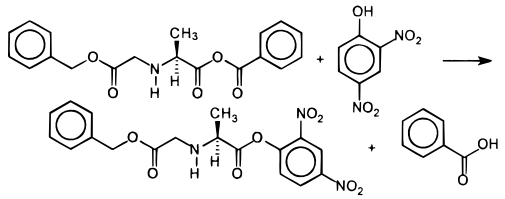	silica	+9.23	$k_{cat}/k_{uncat} = 1.52$	87
M	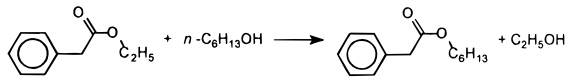	silica	-3.98	not reported	90

[a] k_{cat} = rate constant for the catalyzed reaction system, k_{uncat} = rate constant for the nonimprinted material (polymer or silica) or solution background reaction rate (antibody). [b] AB = antibody, P = polymer; TOF is the turnover frequency. [c] The antibody-catalyzed reaction was analogous to that shown with a substituent group at the δ-carbon. [d] A homogeneous reaction was carried out with phenol–imidazole for comparison. The reported k_{cat}/k_{hom} represents the rate constant of the imprinted polymer divided by that afforded by the homogeneous system.

initio methods to verify the correspondence in bond lengths and angles between the organophosphorous TSA **6** and the transition state for the same reaction.[64] On

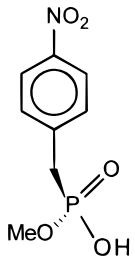

6

imprinting TSA **6** with a polymeric system that was similar to the one used by Robinson and Mosbach, Ohkubo et al. reported a rate acceleration of up to 6.7 times greater than that for the uncatalyzed reaction in 10% methyl sulfoxide in water (pH 7.0). For comparison, a homogeneous catalyst comprised of an imidazole–bisresorcinol derivative was reported to increase the relative rate of *p*-nitrophenyl acetate esterolysis by a factor of approximately 16 over the uncatalyzed reaction in 10% acetonitrile in water (pH 8.2).[67] Ohkubo et al. also calculated the activation enthalpy, entropy, and free energy for the imprinted polymer-catalyzed reaction and the uncatalyzed reaction. However, it is not clear to us what method was used to calculate these thermodynamic state functions. The calculations show that the imprinted polymer stabilized the free energy of the reaction transition-state by only 0.3 kcal/mol over that of the uncatalyzed reaction.[64] This corresponds to a relative rate increase of about 1.6 over the uncatalyzed reaction,[56,57] which is significantly less than the experimentally measured value of 6.7 discussed above. We note that calculations of the activation free energy in a separate system also lead to similar inconsistencies.[68] (Also refer to reaction G in Table 3.) We note that similar mild rate enhancements have been observed in other imprinted polymer-catalyzed reactions and that this trait appears to be common among imprinted polymer catalysts reported to-date.[66,68]

The dehydrofluorination of 4-fluoro-4-(*p*-nitrophenyl)-butan-2-one (reaction D in Table 3 and below) has been conducted with both imprinted polymers and antibody catalysts:[69–71]

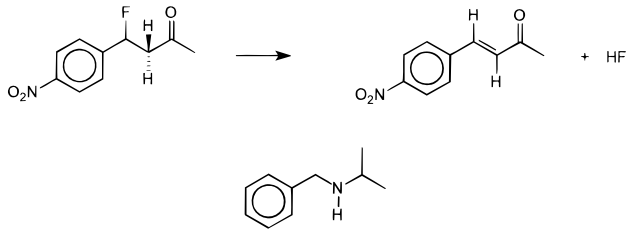

7

Müller et al. prepared an imprinted polymer in acetonitrile with *N*-benzylisopropylamine (**7**) as the transition-state analogue.[69] These workers used the TSA **7** to prepare the catalyst as schematically illustrated in Figure 12. The secondary amine of the TSA probably interacts via a single-point binding with the carboxylic acid group of the binding monomer. This procedure supposedly creates a nanopore with a strategically placed carboxylic acid group that is capable of acid catalyzing the elimination reaction. Despite the apparent simplicity of this one-point binding approach, a factor of 2.4 in the relative rate constant (imprinted polymer rate constant divided by nonimprinted polymer rate constant) was reported between the imprinted and nonimprinted polymers when conducting the elimination reaction in acetonitrile solvent. However, even though the reaction is exothermic (see Table 3), Müller et al. report that product inhibition appears to be a significant problem when conducting the reaction in an aqueous environment, supposedly since both reactant and product adsorbed strongly in a nonspecific manner to the hydrophobic polymer surface. The lack of common solvent between the Müller et al. system and the catalytic antibody system,[71] which was conducted in an aqueous solvent environment, prohibits a direct comparison of the two cases (it is not possible to separate the independent effects of different catalytic approaches and different solvent environments).

A more sophisticated approach to imprinting a polymer catalyst for the elimination reaction involved a two-point binding site.[70] Benzylmalonic acid (**8**) was used

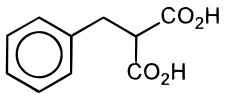

8

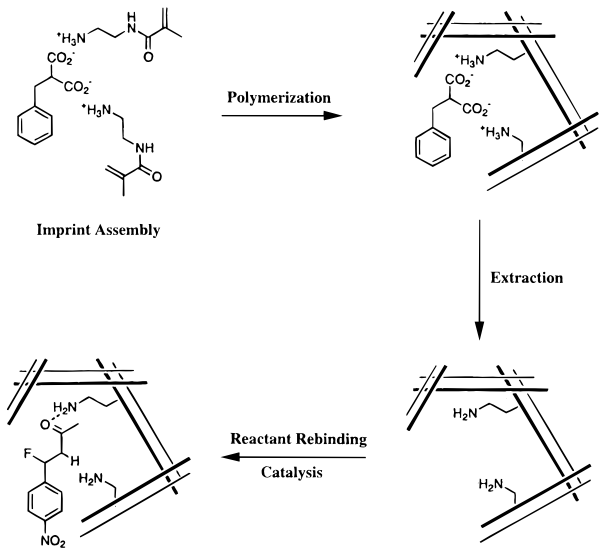

Figure 13. Polymer imprinting scheme used by Beach and Shea for the dehydrofluorination reaction (adapted from ref 70).

Table 4. Dependence of the Beach and Shea Imprinted Polymer-Catalyzed Reaction Rate on Solvent Polarity (Adapted from Ref 70)

solvent	dipole moment[a] (D)	relative rate[b] (k_{cat}/k_{uncat})
acetonitrile	3.92	2.2
ethanol	1.69	1.5
benzene	0	7.5

[a] Data from *CRC Handbook of Chemistry and Physics*, 63rd ed.; Weast, R. C. Ed.; CRC Press: Boca Raton, FL, 1982, pp E59−E61. [b] Relative rate represents rate constant of imprinted polymer catalyst (k_{cat}) divided by the rate constant of nonimprinted polymer catalyst (k_{uncat}).

as the TSA to supposedly position amine functionalities of two binding monomers in each nanopore as schematically illustrated in Figure 13. The concept is that one of the two binding monomers is used to anchor the reactant into the nanopore via the carboxylic oxygen, and the other to bring about the base-catalyzed elimination reaction by providing a basic environment near the α-hydrogen. Note that this approach of providing two binding sites per nanopore increased the relative rate constant by a factor of 1.46 over the Müller et al. one-point binding site approach. Product inhibition similar to that observed by Müller et al. may also have been present in the two-point binding site, since the effect of the imprinted catalysis declined for polar solvents, as shown by the data provided in Table 4. Comparison of the Beach and Shea results with those from a catalytic antibody on the same reaction demonstrate that the rate constant observed in the case of imprinted polymers is significantly lower than that reported for the antibodies.[71] The results of this comparison are summarized in Table 5, where it is shown that the catalytic antibody reveals a Michaelis−Menten binding constant of at least 148 times less and a relative rate constant (see Table 5 for definition) of 198 times larger than the Beach and Shea imprinted polymer.

As with the Müller et al. system, we note that a direct comparison of the antibody and imprinted polymer systems is not warranted in this case, since the imprinted polymer catalysis was conducted in benzene. It is expected, however, that the catalytic antibody binding (and corresponding transition-state stabilization) was

Table 5. Comparison of Catalytic Antibody (Adapted from Ref 71) and Beach and Shea Imprinted Polymer (Adapted from Ref 70) for the Dehydrofluorination Reaction

catalytic system	solvent	relative rate[a] (k_{cat}/k_{uncat})	binding constant (mM)
catalytic antibody	aqueous	1485	0.182
imprinted polymer	benzene	3.5 (unoptimized) 7.5 (optimized)	27 (unoptimized)

[a] Catalytic rate constant, k_{cat}, denotes rate constant with imprinted polymer or antibody. Control rate constant, k_{uncat}, denotes background rate constant of nonimprinted polymer or solution without antibody. Beach and Shea (ref 70) report two different relative rate constants based on optimized and unoptimized reaction conditions.

significantly more specific than for the imprinted polymer, since the antibody did not show product inhibition of the reaction in an aqueous environment as did both imprinted polymer systems. Additionally, the antibody reactivity was completely inhibited by the addition of free hapten, which suggests that the antibody rate accelerations were indeed due to the specific binding afforded by the antibody.[71] Similar types of inhibition experiments with the Beach and Shea imprinted polymer were less conclusive about the role of the imprinted nanopores in the observed catalysis. Upon contacting the imprinted polymer with a 5-fold excess of diethyl benzylmalonate (**9**), the rate of dehydrofluorination

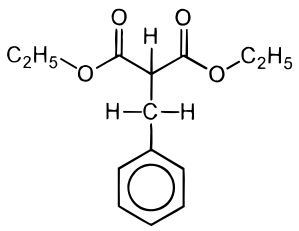

9

dropped only 16%.[70] This small decrease in reaction rate on binding site inhibition raises serious questions as to the nature of the catalytically active sites in the Beach and Shea imprinted polymer. Binding inhibition of the catalytically active sites is not in general a problem with imprinted polymer catalysts, as inhibition experiments on other imprinted polymer systems have shown to fully suppress catalytic turnover.[62,65]

There have also been attempts to impart reaction stereoselectivity with imprinted polymer catalysis. Early studies by Damen and Neckers showed that it is possible to affect the stereochemical direction of the photochemical dimerization of *trans*-cinnamate esters using polymers imprinted with α-truxillic, *β*-truxinic, and *δ*-truxinic acids (see Figure 14).[72] A sample of the catalytic results of Damen and Neckers is shown in Table 6. Note that dimerization of *trans*-cinnamate esters bound to a nonimprinted polymer exclusively formed α-truxillic acid.[72] It does appear that some stereoselectivity is obtained with *β*- and *δ*-truxinic acid imprinted polymer catalysts. More recently, Wulff and Vietmeier obtained a 36% enantiomeric excess for a threonine- and allothreonine-producing reaction.[73] One of the most impressive examples of imprinted polymer catalysis to date is the selective reduction of steroid 3- and 17- (reaction H in Table 3) ketones with $LiAlH_4$ by Byström et al.[74]

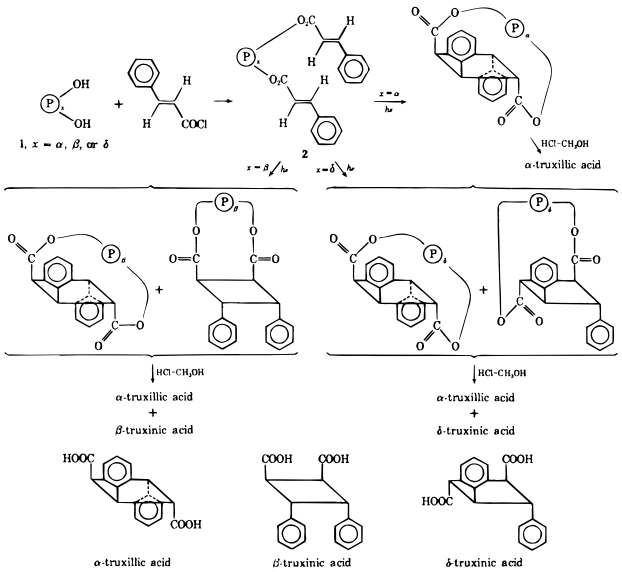

Figure 14. Polymer imprinting and catalysis scheme used by Damen and Neckers for the stereochemical control of the photochemical dimerization of *trans*-cinnamate esters. "P" represents a general imprinted nanopore in the polymer framework. Reprinted with permission from ref 72.

Table 6. Results on the Stereochemical Control of the Photochemical Reaction of *trans*-Cinnamate Ester Using Polymers Imprinted with α-Truxillic, *β*-Truxinic, and *δ*-Truxinic Acids (Adapted from Ref 72)

polymer template	α-truxillic[a]	*β*-truxinic[a]	*δ*-truxinic[a]
α-truxillic acid	100	0	0
β-truxinic acid	47	53	0
δ-truxinic acid	47.3	0	52.7

[a] Stereochemical composition (mol %) of acid in reaction products.

In this example, polymer imprinting was used to selectively place a reactive $LiAlH_4$ group into a nanopore that had the shape of the steroid ketone reactant molecule. The regio- and stereoselectivity of the resulting reduced products could then be controlled to a remarkably high degree, in some cases showing a complete preference for the reduction along the imprinted pathway. Most recently, Sellergren and Shea produced imprinted polymers that were capable of enantioselective ester hydrolysis (reaction I in Table 3).[75] The relative rates of enantiomer production differed by up to a factor of 1.85, thus giving an enantiomeric excess of almost 30%. Note that an antibody catalyst has been reported to conduct a similar amide hydrolysis reaction enantiospecifically.[76]

As described above, there has been a considerable amount of work that attempts to endow imprinted polymers with the binding selectivity of antibodies. In certain cases, the binding selectivity of the imprinted polymer sites approaches that of the antibody. However, for most cases, these selective sites are few and accompanied by a large excess of poorly selective sites. We believe that the fundamental problem in imprinted polymer catalysis is the control of the binding site heterogeneity and this remains as the significant challenge of the future. Several questions that need to be addressed in this regard include what is the driving force for heterogeneous surface formation in these materials and how can this driving force be controlled to give the desired binding site selectivity for a given application? Secondary issues also arise from the existence of site heterogeneity on imprinted polymers. For example, it is not at all clear what the rigorous interpretation of a Lineweaver−Burk plot is for such a truly heterogeneous system. Perhaps calculated values for the kinetic and binding parameters represent average values; correct implementation of the Michaelis−Menten analysis should be limited to a homogeneous surface such as provided by monoclonal antibodies or enzymes.[16]

Next, we discuss another class of amorphous materials for which imprinting has been employed to create catalytic materials, i.e., amorphous silica-based catalysts. The imprinting methods are similar to those described above for polymers and the issues raised previously concerning the polymer-based catalysts must also be addressed with amorphous silica-based catalysts.

Imprinted Amorphous Metal Oxides. Since the pioneering work of Dickey,[8,9] different oxides, such as silicas and mixed metal oxides, have been imprinted in attempts to prepare adsorbents, separation media, and catalysts. To date, amorphous metal oxides have not revealed the same level of success as imprinted polymers for separation and catalytic applications. However, there are drawbacks associated with using polymers as discussed above. In addition, the thermal stability of polymeric systems limits the method of imprint removal to liquid−liquid extraction, which inevitably leaves a small amount of residual imprint in the polymer matrix.[43] The remaining imprint creates uncertainty regarding the mechanism of molecular recognition in the resulting imprinted material. For example, it has been argued that a recrystallization mechanism may be partially responsible for the observed imprinting effect in binding experiments.[9,79,80] On the other hand, with metal oxides, the imprint can be removed virtually completely by harsher techniques such as combustion with dioxygen. Finally, polymers are unsuitable for use in severe industrial environments such as high temperatures and pressures and reactive organic solvents. The use of metal oxides such as silica can overcome these difficulties while expanding the range of materials available for imprinted molecular recognition sites and ultimately selective catalysis.

Wulff and co-workers investigated the binding capabilities of imprinted silicas by using the controlled distance method that was described in the previous section.[45,46] Aryl-bridged cyano compounds **10** and **11**

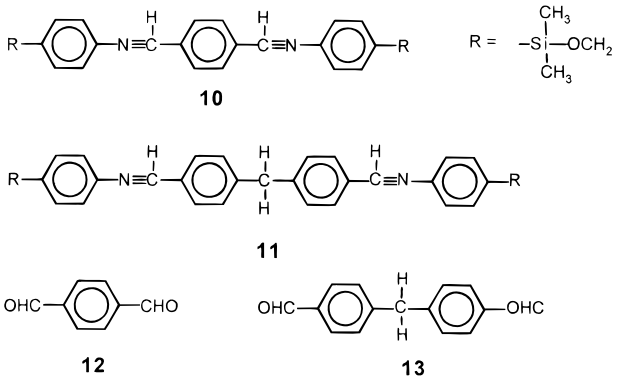

were used to produce positioned amine binding sites by first attaching these species with dimethylmethoxysilane moieties to a silica surface. The bridging groups

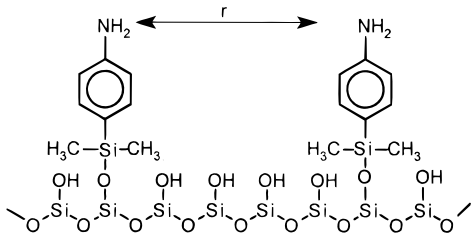

Figure 15. Representation of two amino groups located at a fixed distance, *r*, on the surface of silica formed by cleaving compounds **10** or **11** (adapted from ref 45).

Table 7. Selectivity of Modified Silicas (Adapted from Ref 45)

silica imprinted with	distance *r* (nm)	apparent binding constants with **12**	apparent binding constants with **13**	selectivity (ratio of binding constants)
10	0.72	4.91	2.58	1.74
11	1.05	9.07	13.77	1.67

were subsequently cleaved, leaving behind silica-bound amino groups at well-defined positions and distances from each other (see Figure 15). The surface was then treated with hexamethyldisilazane to minimize nonselective interactions. The binding affinities of the corresponding dialdehydes **12** and **13** were measured. The binding selectivities shown in Table 7 suggest that a slightly preferential binding is possible from the imprinted silica surface. Although the effects are not large, this investigation is the first report of controlled distance binding of an imprint to a silica substrate. Like all previous work on imprinted metal oxides, these studies were limited to investigations involving adsorption alone.

The first example of an imprinted silica used to catalyze a reaction was reported by Morihara and co-workers.[81] Modification of silica by isomorphic substitution of Al^{3+} ions into the silicate matrix was used to generate Lewis acid sites. Morihara and co-workers imprinted an aluminated silica with a TSA for the butanolysis of benzoic anhydride that contained a Lewis base to preferentially bind to the Al^{3+}-active sites. After the gel was aged, the imprint was removed by Soxhlet extraction to supposedly leave behind cavities that are able to catalyze the butanolysis of benzoic anhydride (reaction J in Table 3). This work was aptly termed "footprint catalysis". Morihara's group has since published a series of papers on the subject covering several different reactions. In addition to basic kinetic studies, investigations into competitive inhibition and a limited analysis of the active-site affinities have also been reported.[81−86]

An illustrative example of a "footprint"-catalyzed reaction is the 2,4-dinitrophenolysis of benzoic anhydride (reaction K in Table 3 and below). The reaction was accomplished using catalysts that were imprinted with the TSAs **13**,[83] **14**, and **15**.[85] A selection of reactivity results are shown in Table 8. With imprints **13** and **14**, the relative Michaelis−Menten constant, K_m, decreases over the control material (indicating improved binding) as does the reaction rate constant k_{cat}. A different trend is observed with TSA **15** that contains a tetrahedral phosphorous group. For **15**, the relative binding affinity increases by an order of magnitude and the reaction rate constant increases as well. This suggests that the design of the TSA requires more than

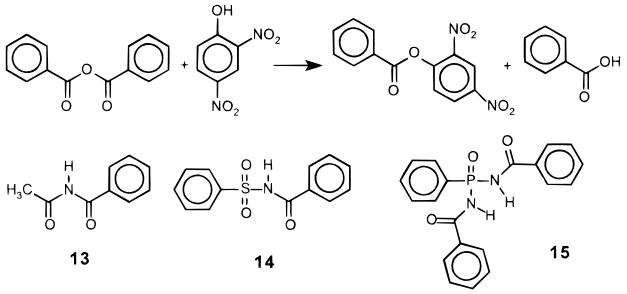

13 **14** **15**

just a simple gross structural match between the transition state and its analogue, since all of the imprints are structurally similar. We investigated these results further by assessing the Lewis basicity of the imprints using molecular mechanics calculations.[59] (Recall that the footprints are formed by preferential binding of a Lewis base to the Al^{3+} sites during the imprinting process.) The results of this molecular mechanics calculation, which are shown in the last column of Table 8, demonstrate that TSA **15** contains the strongest Lewis base and hence is more likely to produce a stronger interaction, i.e., an imprint site, than TSAs **13** and **14**. This observation may explain the enhanced substrate specificity observed with this compound. Morihara and co-workers also report inhibition of the reaction on addition of the corresponding TSAs; however, turnover is never suppressed completely in these inhibition studies, so only a limited conclusion about the activity of the imprinted sites can be drawn.

In a demonstration of chiral recognition, Morihara and co-workers imprinted, *N*-benzoyl-(N^{α}-benzyloxycarbonyl)-*l*-alaninamide (**16**) onto an Al^{3+}-doped silica gel[87]

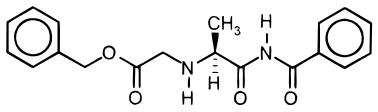

16

(see Figure 16). This imprinted catalyst was used to catalyze the enantioselective 2,4-dinitrophenolysis of *N*-benzyloxycarbonyl-*l*-alanine anhydride (**17**, reaction L in Table 3 and below):

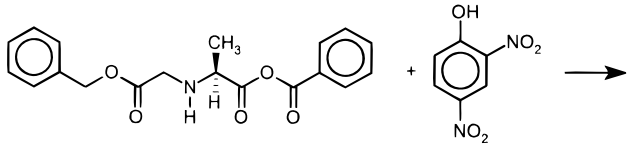

17

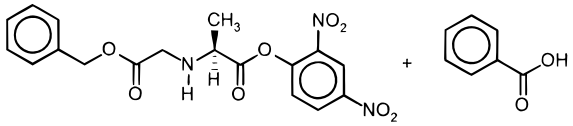

Kinetic resolution was reported. The enantioselectivity was explained by a productive and nonproductive binding mechanism as illustrated in Figure 16.[88,89] Chiral imprint **16** produces three subsites in the aluminated silica substrate corresponding to residues of the alanine substructure. Productive binding is speculated to occur only with the *l*-enantiomer that places **17** in a favorable conformation on the acid site of the silica for nucleophilic

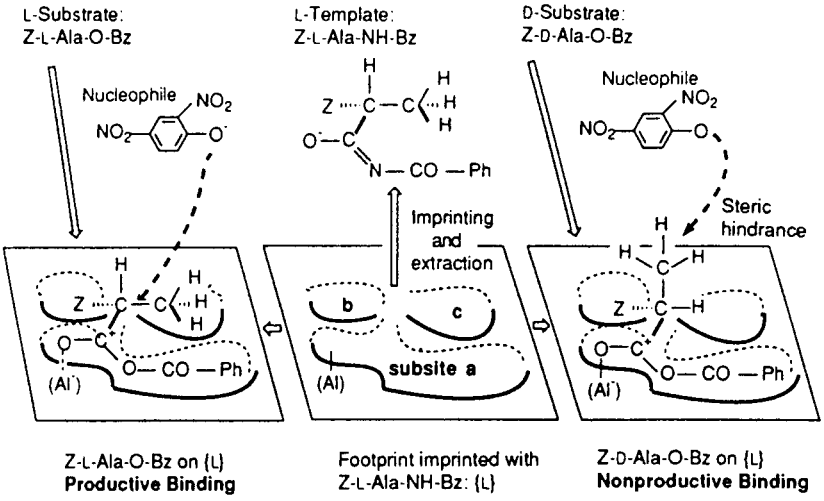

Figure 16. Proposed mechanism of enantioselectivity for the 2,4-dinitrophenolysis of **17**: chiral *l* molecular footprints are produced by **16** and consist of three sites denoted a, b, and c corresponding to substructures −CO−NH−Bz, Z−NH−, and methyl (not α-hydrogen) of the alanine residue. Productive binding: The *l* substrate binds to the footprint through a three-point interaction maintaining the same α-methyl configuration as the imprint; this places the carbonyl group of the reaction center for activation on the Lewis acid site (Al), thus allowing transformation by nucleophilic attack with 2,4-dinitrophenoxide. Nonproductive binding: The *d* substrate binds to the footprint through another three-point adsorption as in (b) except that the hydrophobic α-hydrogen replaces the methyl group. Consequently the methyl groups shield the carbonyl compound from nucleophilic attack. The abbreviations refer to the following moieties:

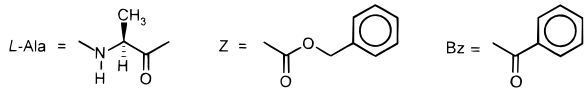

Reprinted with permission from ref 87. Copyright 1992 The Royal Society of Chemistry.

Table 8. Kinetic Parameters for the 2,4-Dinitrophenolysis of Benzoic Anhydride (Adapted from Refs 83 and 85) and Imprint Oxygen Lewis Basicities

catalyst imprinted with	$10^{-2}k_{cat}$[a] (M^{-1} s^{-1})	$10^{4}K_m$[b] (M)	$10^{-5}k_{cat}/K_m$ (M^{-2} s^{-1})	charge on benzoyl oxygen[c]
13	1.89	2.70	7.00	−0.481
14	4.04	3.36	12.02	−0.478
15	33.36	4.06	82.23	−0.478, −0.534
control (no imprint)	6.79	18.0	3.77	

[a] k_{cat} = rate constant for the catalyzed reaction. [b] K_m = Michaelis constant. [c] Equilibrium charge on imprint oxygen determined using the Dreiding force field[59b] algorithm in the Cerius[2] software package.

attack by the dinitrophenoxide. The *d*-enantiomer cannot undergo the same reaction since it is sterically hindered by the methyl group.

Although Morihara and his group have achieved some success in imprinting amorphous oxides for catalysis, several significant limitations remain that need to be overcome in order to achieve the efficacy of catalytic antibodies. The most significant problems that need to be addressed are the low enhancements of catalytic activity, poor selectivity, and long-term stability. This could be largely due to the heterogeneity of the catalytic sites. Moreover, the aluminum dopant used is itself a catalytically active site for these reactions. Thus, it is unclear as to what fraction of the catalysis is indeed attributable to the imprinted sites in the silica. Further characterization of the active sites is therefore necessary to address this issue. It should also be pointed out that many of the "footprint"-catalyzed reactions release organic acids, and these may provide for autocatalysis. This underscores the need for additional control experiments. In view of the Hammond postulate discussed in the previous section, we believe that the low reported activities may be largely attributable to product inhibition due to the endothermicity of reactions K and L (listed in Table 3).

Using a different approach, Heilmann and Maier recently reported a selective silica catalyst for the transesterification of ethyl phenylacetate to hexyl phenylacetate[90] (reaction M in Table 3). This reaction normally occurs only with measurable rates in the presence of acid or base catalysts. A possible transition-state for the acid-catalyzed reaction **18** was used in

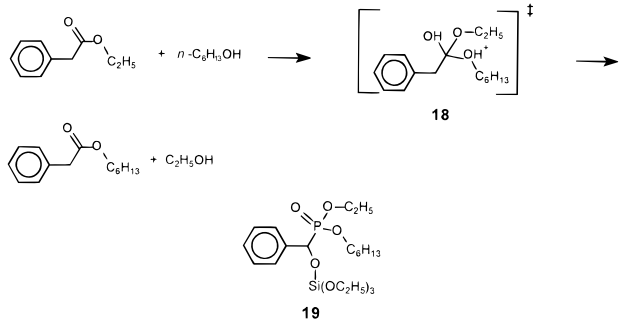

designing **19** as a TSA. The copolymerizable triethoxysiloxy moiety on **19** was employed to chemically bind the TSA into the silica gel during an acid-catalyzed sol−gel process with a 100-fold molar excess of the monomer $Si(OEt)_4$ (similar to the self-assembly method described previously for imprinted polymer synthesis). Heilmann and Maier remove the TSA by combustion in air to supposedly leave behind a silica-based solid with well-defined three-dimensional cavities (supposedly, phosphorous remains on the silica and is the active site for the catalysis). They claim that since the TSA is covalently attached to the silica prior to calcination, this imprinting procedure is more robust than the approach

of Morihara et al.[81−87] Heilmann and Maier observed that the transesterification reaction was catalyzed by the imprinted solid and as a test for the selectivity of the imprinted site, the rates of transesterification of ethyl napthylacetate vs ethyl phenylacetate were investigated. No reaction was reported when using the napthyl compound. They also reported that the catalyst was able to discriminate between hexyl and phenyl alcohols for the transesterification reaction. The success of their catalyst was attributed to three-dimensional imprinted cavities containing acid sites.[90]

The promising results of Heilmann and Maier motivated us to further investigate this system.[91] We observed comparable rate enhancements for both the napthyl and phenyl esters and no inhibition of the reaction using the selective inhibitor **20**. In our investigation, we were unable to find evidence for molecular recognition and catalysis from an imprinted site.

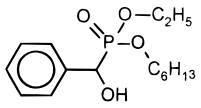

20

In a report of an antibody-catalyzed unimolecular reaction, Benkovic and co-workers elicited a monoclonal antibody against the stable TSA **21** (cf. **22a**) of an intramolecular six-membered ring-cyclization reaction that was capable of stereospecific catalysis.[92] A single enantiomer of δ-lactone **23a** from a racemic mixture of δ-hydroxy ester **24a** was formed with a 167-fold rate

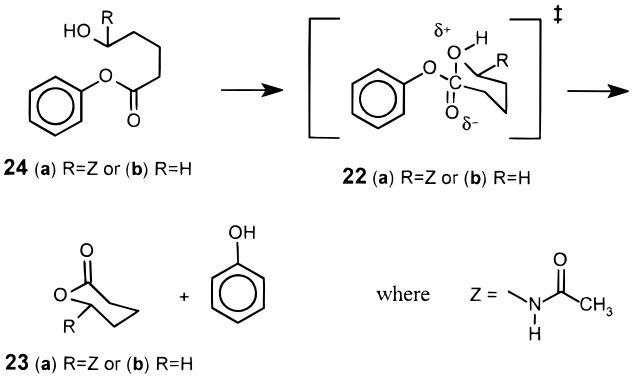

24 (**a**) R=Z or (**b**) R=H

22 (**a**) R=Z or (**b**) R=H

23 (**a**) R=Z or (**b**) R=H

where Z =

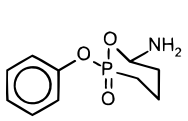

21

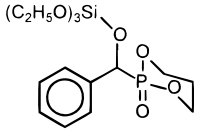

25

acceleration to give an enantiomeric excess of 94% (analogous to reaction E in Table 3). Inhibition of the catalyzed reaction was observed to occur linearly with the addition of **21**. Motivated by these significant results, Heilmann and Maier followed a procedure analogous to that described above for the transesterification reaction to prepare an imprinted silica catalyst for the achiral intramolecular lactonization reaction of **24b** to **23b**. Heilmann and Maier used the TSA **25** to imprint the silica[93] (cf. **22b** and reaction E in Table 3). The catalyst reportedly accelerated the intramolecular lactonization; however, control experiments revealed that the enhancement in activity was not attributable to the imprinted cavity.

Like the imprinted polymers, imprinted amorphous metal oxides have shown some indication of catalysis that can be attributed to the imprinting process. However, it appears that site heterogeneities are prevalent and limit reaction selectivities. Next, we discuss crystalline metal oxides that have significantly less site heterogeneity than either polymers or amorphous metal oxides.

Zeolites

Zeolites are *crystalline* aluminosilicates that have pore sizes in the range 2−10 Å. Because these metal oxide materials are not amorphous, they can have very uniform pore-size distributions that are fixed by the atomic arrangements of their unit cells (repeat unit of the crystal). The existence of nonvarying pore diameters that are in the size range of small molecules endows zeolites with extraordinary molecular discrimination abilities. For example, zeolite A can adsorb linear paraffins while rejecting branched hydrocarbons, e.g., *n*-butane vs isobutane. The difference in kinetic diameter between the two butane isomers is 0.3 Å. Thus, zeolites have been called molecular sieves for obvious reasons. A brief review of zeolites can be found elsewhere.[94]

There is a close connection between the nanometer scale structure and the macroscopic properties of zeolite catalysts. Venuto has recently provided an exhaustive review (579 references) on the catalysis of organic molecules over zeolite catalysts.[95] Thus, it is obvious that we cannot provide an overview of all catalysis over zeolites because the field is so large; here we will limit our discussions to those issues relevant to the theme of this review. In general, the continuing commercial successes of zeolite catalysts are largely due to the constant discovery of new materials that enables process improvements and the development of new technologies. The ability to control the zeolite properties through synthetic efforts is and will continue to be of great importance. At present, the control of zeolite properties mainly involves molecular level manipulations of structural features, e.g., pore size and location of active sites.[96] That is to say, the chemical and/or electronic nature of the catalytically active site is not normally controlled. Rather, the three-dimensional structure surrounding the active site is fabricated.[97] In the 1970s and 1980s, "catalyst design" with solid materials normally implied the manipulation of the porous solid material to affect the mass- and energy-transport properties of the catalyst (length scales of 10^{-2}−10^{-8} m). Today, with zeolite catalysts, "design" implies manipulation at the nanometer-to-angstrom length scale and involves the complementarity between the active site and reactant/product geometries.[97]

Zeolite catalysis has centered around shape-selective, acid-mediated reactions. Zeolites are anionic oxide structures that require cations for maintaining electrical neutrality (the amount of the anionic sites are on the order of mequiv/g of zeolite). If the balancing cation is a proton, then the zeolite can function as a solid acid catalyst. Since these sites are contained within the pore space of the zeolite crystal, access to these catalytic sites

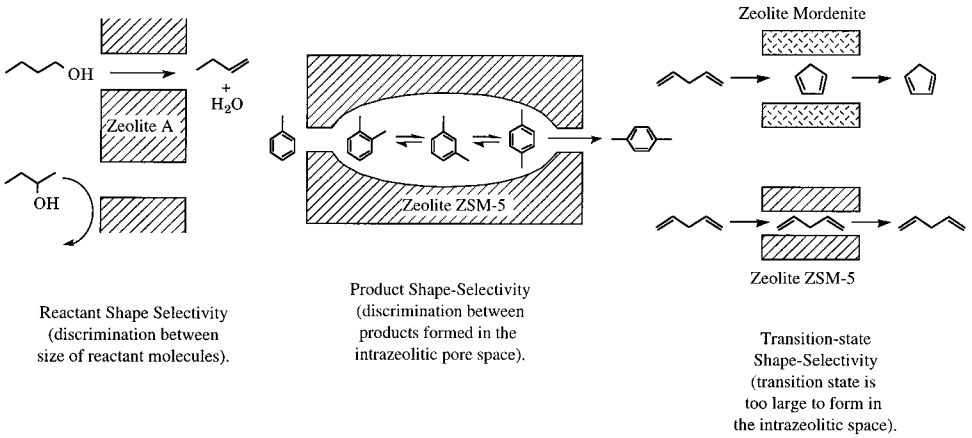

Figure 17. Schematic representations of the types of primary shape selectivity.

is through the subnanometer-sized pores. This is why zeolites can perform shape-selective catalysis. The primary forms of shape-selective catalysis are illustrated in Figure 17 and are reactant, product, and transition-state selectivity.[98] For a short review on primary and secondary shape-selective catalysis with zeolites, see ref 102. Here, it is sufficient to illustrate only primary shape-selective catalysis. Reactant and product shape selectivity involve molecular discrimination between reactant and product molecules, respectively. There are numerous examples of reactant shape selectivity, and this type of catalysis is easy to recognize and test for, i.e., by measuring the catalytic activity for a series of reactants of varying size. Product shape selectivity can be observed, and the most studied example is the synthesis of near-pure *p*-xylene from toluene over ZSM-5-based catalysts. With product shape selectivity, several products are formed within the zeolite pore space and are able to convert into each other. At least one of the products has a smaller kinetic diameter than the others, and therefore it diffuses through the zeolite pores at a higher rate than the other products. As the fast diffusing species moves out of the zeolite crystals, the other compounds convert to this species (thus allowing the catalysis to continue; if interconversion were not possible, then the larger molecules would clog the zeolite pore space). A good test for the existence of product shape-selectivity is to monitor the product distribution as a function of increasing the zeolite crystal size; the larger the crystal, the greater the selectivity to the faster diffusing species.

To date, proven examples of transition-state shape selectivity are rare. The example illustrated in Figure 17 shows that the cyclization of dienes can take place in the zeolite mordenite while no reaction occurs in ZSM-5 even though there are active sites available to perform the reaction. This is due to a lack of sufficient pore space to form the transition state since cyclopentadiene will adsorb into the pores of ZSM-5. Oftentimes the lack of a particular product, e.g., one of the trimethylbenzenes in the disproportionation of *m*-xylene, is construed as evidence for transition-state shape selectivity. However, selectivities of this type can result from product shape selectivity as well. Thus, one test to distinguish between transition state and product shape selectivity is to observe the product distribution as the crystal size is varied; there should be no variation in the product composition if transition-state shape selectivity is the controlling process, while such is not

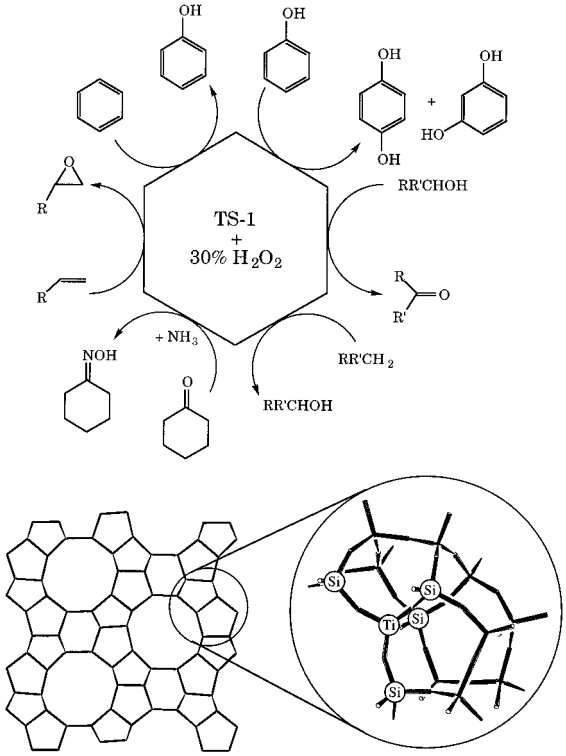

Figure 18. Types of reactions catalyzed by TS-1 (schematic of titanium site in TS-1 is provided also).

the case with product-shape selectivity. In conclusion, significant progress has been made in rationally developing zeolite catalysts that function via reactant shape selectivity and to some extent with product shape selectivity. However, very little work has concentrated on the purposeful use of transition-state selectivity.

In addition to acid-mediated catalysis with zeolites, base catalysis and oxidation chemistries are now performed with zeolites.[97] A particularly germane example for this review is the oxidation catalysis by the use of the titanosilicate TS-1 (has the structure of ZSM-5).[103,104] TS-1 is the pure-silica version of the zeolite ZSM-5 in which ~1−2 atom % of the silicon atoms are substituted by tetravalent titanium atoms. This material is capable of catalyzing a very broad spectrum of oxidation reactions (see Figure 18) using aqueous H_2O_2 as the oxidant at temperatures below 373 K. TS-1 has revolutionized zeolite catalysis, and one reason for doing so is that it demonstrated that low-temperature liquid-phase reactions are commercially feasible with a zeolite-

based catalyst (phenol to hydroquinone and catechol and cyclohexanone to the oxime are now both practiced on commercial scale and the epoxidation of olefins is near commercialization). TS-1 is able to accomplish these chemistries using aqueous H_2O_2 as the oxidant. It is well-known that titanium compounds are not able to catalyze oxidation reactions if water is present, e.g., the Sharpless asymmetric, homogeneous epoxidation of allyl alcohols and Shell's heterogeneous titanium on amorphous silica catalyst for propylene epoxidation. How is it that TS-1 is able to remain active in the presence of water? Khouw et al. addressed this issue.[105] TS-1 is hydrophobic. Organic reactants are adsorbed into the hydrophobic pore space, oxidized, and displaced by other reactant molecules. That is to say, the more hydrophobic reactants partition from the bulk solution phase into the hydrophobic pore space and in doing so readily displace products (more hydrophilic since they are oxidized forms of the reactant) and water (from the H_2O_2) back into the bulk solvent phase. This behavior is similar to that observed in certain enzymes, i.e., partitioning of substrates from the aqueous solution to the hydrophobic active site that excludes water and then releases the product back to the aqueous phase, e.g., methane to methanol with methane monooxygenase. Thus, in addition to shape selectivity, it is possible to control the partitioning of reactants/products from the solvent to the intrazeolitic reaction site by tuning the hydrophilic/hydrophobic nature of the zeolite.[106]

Zeolites can be synthesized using organic molecules as "templates." As pointed out by Davis and Lobo, the specificity between the organic guest and the zeolite host is as yet not sufficient to invoke true templating in the sense that this term is used in biological contexts.[96] Here, we will call the organic species structure-directing agents (SDAs) since they have been shown to dictate the final outcome of a zeolite synthesis. Figure 19 illustrates a schematic of a reasonable proposal for the synthesis of a zeolite (ZSM-5) that employs a SDA (tetrapropylammonium cation, TPA).[107] Initially, the hydrophobic hydration sphere of TPA is partially or completely replaced by silicate species. Favorable van der Waals contacts between the alkyl groups of the TPA and the hydrophobic silicate species likely provide the enthalpic driving force while release of ordered water to the bulk aqueous phase provides an additional entropic driving force for the assembly process.[108] It is via these organic−inorganic interactions that the geometric correspondence between the organic SDA and the zeolite pore architecture arises.[96,107−109] These composite species have recently been identified by NMR techniques[107] and trapped by silylation methods.[107b] The organic−inorganic species then combine to form entities of size around 5−7 nm (identified by in situ SAXS[110] and cryo-TEM[111] studies). These nanostructured entities are proposed to be the nucleation sites for crystal growth.[112] A complete discussion of the mechanistic details and references for the experimental evidence supporting the proposal shown here can be found elsewhere.[112] What is important about this type of zeolite synthesis (in the context of this review) is that the inorganic species are organized by the organic molecules via numerous noncovalent, i.e., weak, interactions that ultimately determine the kinetic pathway of the crystallization process (all zeolites are metastable

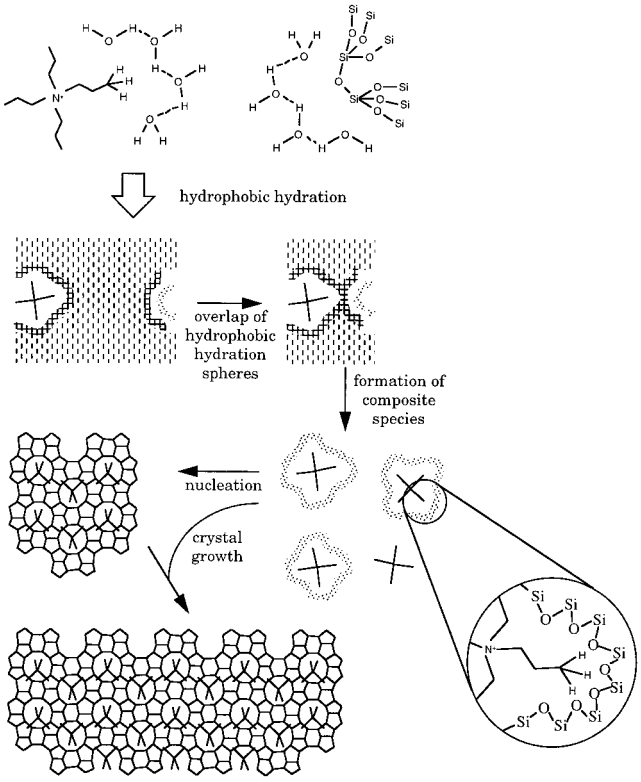

Figure 19. Schematic of proposed mechanism for the synthesis of ZSM-5 (adapted from ref 107).

phases that are produced by kinetically controlled synthetic processes). Thus, like the self-assembly processes for amorphous "imprinted" materials (see previous sections), zeolite synthesis employs relatively weak, noncovalent intermolecular interactions to direct the synthesis.

It is obvious that not just any organic molecule can serve as a SDA for zeolite synthesis. The properties necessary for structure direction to occur in the synthesis of high-silica zeolites have been discussed previously.[96,108,113] What is clear from the organics that have been shown to function as SDAs is that they have intermediate hydrophobicity.[107] Presumably this allows the organics to remain as isolated molecules in aqueous solutions with hydrophobic hydration spheres.[107] If the organic molecules interact too strongly with water, then silica can never be organized by the organic species.[107c]

Although a complete mechanistic picture is not available, the known general features of the assembly process lead to strategies for zeolite synthesis by design.[112] Demonstrated examples of designing SDAs to product desired zeolite pore architectures exist.[114,115] An interesting example of the design of zeolite pore architecture is due to Zones and co-workers.[114] Using the linear diquaternary ammonium cation shown in Figure 20, Zones prepared a zeolite that contains linear nonintersecting pores (in the as-prepared material the diquat is the guest species in the pores). To force the synthesis to produce a zeolite with intersecting pores, Zones added another ring to the diquat to "break the symmetry" of the molecule about the long axis of the diquat. In doing so, linear nonintersecting pores are not able to form and a new zeolite with intersecting pores was formed by a priori design of the SDA. Additionally, a single attempt to not only control the pore space geometry but also the

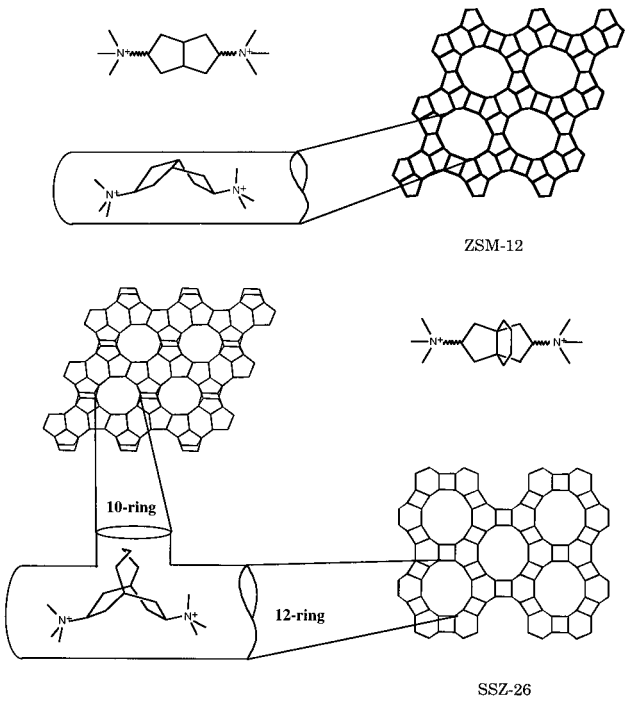

Figure 20. Schematic representations of organic SDAs and zeolites formed (adapted from ref 114).

placement of atoms into specific crystallographic sites has been reported.[116]

Returning to the objective of prepared zeolite catalysts by design, to date there is no clear example of a zeolite catalyst that was prepared by a priori design. However, this goal is being pursued by numerous groups throughout the world. Although zeolites can be prepared via the use of SDAs, no use of a TSA−SDA has appeared. One obvious limitation to the use of a TSA−SDA with zeolites compared to amorphous materials is that the amorphous materials have more conformations available for maximizing guest−host interactions since they are not constrained by symmetry as in the case of a crystalline solid like a zeolite. Regardless, future work on a priori design of zeolite catalysts needs to concentrate further on exploiting transition-state selectivity, and this will require not only the successful construction of the pore architecture but also the placement of the catalytically active element. Initial efforts in one important subarea of the overall concept have appeared. Arhancet and Davis have prepared the first zeolite to show chiral properties. Zeolite β is an intergrowth of two crystal types, one of which can form an enantiomorphic pair. Arhancet and Davis used a chiral SDA to produce a zeolite β that had a very slight enrichment in one of the enantiomorphs, and this material revealed asymmetric catalysis with low enantiomeric excess.[96] These results show that in principle, a chiral zeolite catalyst can be prepared. Lobo and Davis also demonstrated that zeolite materials with chirality should be able to exist and not form intergrowths; i.e., a zeolite analogous to *d*,*l*-quartz. Again, it is expected that a chiral SDA would be necessary to prepare a single enantiomorph. Thus, we believe the potential is high for the synthesis of new zeolite-based catalysts by rational design and believe that if such is done it will exploit transition-state shape selectivity rather than the more traditional reactant and product shape selectivities.

Comparisons

From the aforementioned discussions on catalytic antibodies, imprinted polymers, imprinted amorphous metal oxides, and zeolites, it is clear that each catalytic system contains advantages and disadvantages when considering their use as commercially viable catalysts. Here, we compare and contrast these materials.

Tables 9 and 10 list comparisons between the various imprinted catalytic systems described in this review. The antibody catalyst can show high activity and selectivity that can be attributed to the imprinting process via a TSA imprint. Although the activity is not as high as with enzymes, it can be more than sufficient for practical application in numerous circumstances. The difficulties with antibody catalysts are their preparation methods, their "robustness" (lack of stability in harsh chemical and/or physical environments) and their low productivity. Here, we denote productivity as the product formed per unit volume of reactor. Although antibody catalysts show high turnover frequencies, the concentrations of the reactants are normally very low and the possible regeneration of the catalyst is currently unknown. Thus, catalytic antibodies will likely find use in small-scale syntheses where high selectivities are required.

Imprinted polymer catalysts can yield higher productivities and catalyst "robustness" than catalytic antibodies. However, the polymer catalysts thus far have shown low reaction rates. The imprinted polymers typically reveal low number densities of active sites and site heterogeneity. If the imprinted sites had a significantly higher turnover frequency relative to the nonimprinted sites, then site heterogeneity need not be such a significant issue. The problem is that to obtain high

Table 9. Comparisons of Imprinted Catalysts: Overall Behavior

catalyst type	ease of preparation	"robustness"	regeneration	asymmetric conversions	reaction rates	productivity
antibody	difficult	low	unknown	proven	can be high	low
polymer	moderate	moderate	proven	proven	low	low
amorphous metal oxide	moderate	moderate	unknown	questionable	low	low
zeolite	moderate	high	excellent	questionable	can be high	good

Table 10. Comparison of Imprinted Catalysts: Catalyst Properties

catalyst type	TSA concept of selectivity	range of functionalities for active site	active-site density of catalyst	active-site homogeneity	active-site density in reactor
antibody	proven	broad	high	excellent	low
polymer	likely	broad	low	poor	moderate
amorphous metal oxide	questionable	narrow	low	poor	moderate
zeolite	no	narrow	high	good	high

catalytic activity, a high binding affinity is likely necessary in these materials. A high binding affinity without flexibility around the catalytic site would likely lead to low activity (refer to enzyme model of induced fit) since it would be very difficult to design an appropriate TSA to give high binding without product inhibition (see previous discussions on endothermic vs exothermic reactions). Thus, a better strategy is most likely to prepare imprinted polymers of greater homogeneity with a controlled transition-state stabilization that minimizes product inhibition.

Imprinted amorphous metal oxides show nearly the same features and suffer from the same problems as the imprinted polymers except that the metal oxides do not have the range of functional groups available with polymers to create active sites without grafting of other moieties onto the surface of the metal oxides; only hydroxyl groups and Lewis acid centers (for example, tricoordinated Al^{3+}) are available as catalytic sites.

Zeolites reveal numerous properties that allow them to be commercially viable catalysts, e.g., high active-site density, "robustness", and shape selectivity. However the design of a zeolite catalyst via a TSA has not occurred. Although there are limited examples of transition-state shape-selective catalysis with zeolites, none of these were designed a priori. The limitations imposed by the crystalline nature of zeolites will likely impede the use of the TSA imprinting methodology. Additionally, zeolites suffer from the same lack of functional groups as described for amorphous metal oxides. Despite these shortcomings, zeolites are and will probably continue to be one of the most important materials used commercially as catalysts. However, there will be numerous reactions where the zeolite does not contain the appropriate functional group for catalytic action and/or the selectivity, e.g., pore size and enantioselectivity, necessary for application. It is for these reasons that the aforementioned imprinted systems may prove useful.

Throughout this review we have discussed the positive and negative features of using TSA imprints to synthesize catalytic materials. It is clear from this presentation that the TSA paradigm in imprinting materials for catalysis is alive and well. However, as with other newly developing fields, the number of control experiments and direct comparisons between different catalytic materials still needs improvement. We expect these shortcomings to disappear as the field matures. As we look to the future, the target of mimicking enzyme catalysis appears closer due to continued improvements on the synthesis of nanostructured materials.

Acknowledgment. A.K. is supported by a Fannie and John Hertz Foundation Fellowship. W.R.A. gratefully acknowledges the financial support of Hoechst-Celanese. We would also like to thank Dr. Mario Blanco of the Materials and Process Simulations Center at Caltech for assistance with the molecular mechanics calculations.

References

(1) Wulff, G. *ACS Symp. Ser.* **1986**, *308*, 186.
(2) Shea, K. J. *Trends Polym. Sci.* **1994**, *2*, 166.
(3) (a) Mosbach, K. *Trends Biochem. Sci.* **1994**, *19*, 9. (b) Mosbach, K; Ramström, O. *Bio/Technology* **1996**, *14*, 163.
(4) Kempe, M.; Mosbach, K. *J. Chromatogr.* **1995**, *694*, 3.
(5) Vidyasankar, S.; Arnold, F. H. *Curr. Op. Biotech.* **1995**, *6*, 218.
(6) *Chem. Eng. News* **1949**, *27(13)*, 913.
(7) Pauling, L. *J. Am. Chem. Soc.* **1940**, *62*, 2643.
(8) Dickey, F. H. *Proc. Natl. Acad. Sci. U.S.A.* **1949**, *35*, 227.
(9) Dickey, F. H. *J. Phys. Chem.* **1955**, *59*, 695.
(10) Haldeman, R. G.; Emmett, P. H. *J. Phys. Chem.* **1955**, *59*, 1039.
(11) Curti, R.; Colombo, U. *J. Am. Chem. Soc.* **1952**, *74*, 3961.
(12) Wulff, G.; Sarhan, A. *Angew. Chem., Int. Ed. Engl.* **1972**, *11*, 341.
(13) Fischer, E. *Ber. Dtsch. Chem. Ges.* **1890**, *23*, 2611.
(14) Koshland, D. E. Jr. *Proc. Natl. Acad. Sci. U.S.A.* **1958**, *44*, 98.
(15) Koshland, D. E. Jr. *Angew Chem., Int. Ed. Engl.* **1994**, *33*, 2375.
(16) (a) Fersht, A. *Enzyme Structure and Mechanism*, 2nd ed.; W. H. Freeman: New York, 1985. (b) Creighton, T. E. *Proteins: Structure and Molecular Properties*, 2nd ed.; W. H. Freeman: New York, 1993.
(17) Gerstein, M.; Lesk, A. M.; Chothia, C. *Biochemistry* **1994**, *33*, 6739.
(18) Affleck, R.; Xu, Z. F.; Suzawa, V.; Focht, K.; Clark, D. S.; Dordick, J. S. *Proc. Natl. Acad. Sci. U.S.A.* **1992**, *89*, 1100.
(19) Pauling, L. *Chem. Eng. News* **1946**, *24*, 1375.
(20) Radzicka, A.; Wolfenden, R. *Science* **1995**, *267*, 90.
(21) (a) Boudart, M. *Chem. Rev.* **1995**, *95*, 661. (b) Weisz, P. *CHEMTECH* **1982**, *22*, 424.
(22) Pauling, L. *Am. Sci.* **1948**, *36*, 51.
(23) Tramontano, A.; Janda, K. O.; Lerner, R. A. *Science* **1986**, *234*, 1566.
(24) Pollack, S. J.; Jacobs, J. W.; Schultz, P. G. *Science* **1986**, *234*, 1570.
(25) Schultz, P. G.; Lerner, R. A. *Acc. Chem. Res.* **1993**, *26*, 391.
(26) Schultz, P. *Acc. Chem. Res.* **1989**, *22*, 287.
(27) Schultz, P.; Lerner, R. A.; Benkovic, S. J. *Chem. Eng. News* **1990**, *68*(22), 26.
(28) Stewart, J. D.; Liotta, L. J.; Benkovic, S. J. *Acc. Chem. Res.* **1993**, *26*, 396.
(29) Schultz, P. G.; Lerner, R. A. *Science* **1995**, *269*, 1835.
(30) Haynes, M. R.; Stura, E. A.; Hilvert, D.; Wilson, I. A. *Science* **1994**, *263*, 646.
(31) Hilvert, D.; Carpenter, S. H.; Nared, K. D.; Auditor, M. T. M. *Proc. Natl. Acad. Sci. U.S.A.* **1989**, *85*, 4953.
(32) Hilvert, D.; Nared, K. D. *J. Am. Chem. Soc.* **1988**, *110*, 5593.
(33) Jackson, D. Y.; Liang, M. N.; Bartlett, P. A.; Schultz, P. G. *Angew. Chem., Int. Ed. Engl.* **1992**, *31*, 182.
(34) Chook, Y. M.; Ke, H.; Lipscomb, W. N. *Proc. Natl. Acad. Sci. U.S.A.* **1993**, *90*, 8600.
(35) Thorn, S. N.; Daniels, R. G.; Auditor, M. T. M.; Hilvert, D. *Nature* **1995**, *373*, 228.
(36) Kemp, D. S.; Cox, D. D.; Paul, K. G. *J. Am. Chem. Soc.* **1975**, *97*, 7312.
(37) Stewart, J. D.; Benkovic, S. J. *Nature* **1995**, *375*, 388.
(38) Shevlin, G. S.; Hilton, S.; Janda, K. D. *Bioorg. Med. Chem. Lett.* **1994**, *4*, 297.
(39) Wulff, G. *Angew. Chem., Int. Ed. Engl.* **1995**, *34*, 1812.
(40) Whitcombe, M. J.; Rodriguez, M. E.; Villar, P.; Vulfson, E. *J. Am. Chem. Soc.* **1995**, *117*, 7105.
(41) (a) Kempe, M.; Mosbach, K. *J. Chromatogr.* **1995**, *691*, 317. (b) Kempe, M.; Mosbach, K. *Int. J. Peptide Protein Res.* **1994**, *44*, 603. (c) Ramström, O.; Nicholls, I. A.; Mosbach, K. *Tetrahedron A* **1994**, *4*, 649. (d) Sellergren, B. Ph.D. Thesis, University of Lund, Sweden, 1988. (e) Andersson, L. I. Ph.D. Thesis, University of Lund, Sweden, 1990. (f) Norrlöw, O. Ph.D. Thesis, University of Lund, Sweden, 1986. (g) Kempe, M. Ph.D. Thesis, University of Lund, Sweden, 1994. (h) Fischer, L.; Müller, R.; Ekberg, B.; Mosbach K. *J. Am. Chem. Soc.* **1991**, *113*, 9358.
(42) (a) Hunter, L. *Prog. Stereochem.* **1954**, *1*, 222. (b) Pimentel, G. C.; McClellan, A. I. *The Hydrogen Bond*; W. H. Freeman: New York, 1960.
(43) Sellergren, B.; Shea, K. J. *J. Chromatogr.* **1993**, *635*, 31.
(44) (a) Tao Y.; Ho, T. *J. Chem. Soc., Chem. Commun.* **1988**, 417. (b) Norrlöw, O.; Månsson, M. O.; Mosbach, K. *J. Chromatogr.* **1987**, *396*, 374.
(45) Wulff, G.; Heide, B.; Helfmeier, G. *J. Am. Chem. Soc.* **1986**, *108*, 1089.
(46) Wulff, G.; Heide, B.; Helfmeier, G. *React. Polym.* **1987**, *6*, 299.
(47) Adamson, A. W. *Physical Chemistry of Surfaces*; John Wiley & Sons: Toronto, 1976.
(48) Sellergren, B. *Makromol. Chem.* **1989**, *190*, 2703.
(49) Sellergren, B.; Shea, K. J. *J. Chromatogr.* **1995**, *690*, 29.
(50) Andersson, L. I.; Müller, R.; Vlatakis, G.; Mosbach, K. *Proc. Natl. Acad. Sci. U.S.A.* **1995**, *92*, 4788.
(51) Shea, K. J.; Sasaki, D. Y. *J. Am. Chem. Soc.* **1991**, *113*, 4109.
(52) Sellergren, B. *Chirality* **1989**, *1*, 63.
(53) Mosbach, K. *Protein Engr.* **1995**, *8 (supplement)*, 54.
(54) Andersson, L. I.; Nicholls, I. A.; Mosbach, K. *ACS Symp. Ser.* **1995**, *586*, 89.
(55) Vlatakis, G.; Andersson, L. I.; Müller, R.; Mosbach, K. *Nature* **1993**, *361*, 645.
(56) Levine, I. N. *Physical Chemistry*, 3rd ed.; McGraw Hill: New York, 1988.

(57) Jencks, W. P. *Catalysis in Chemistry and Enzymology*; Dover: New York, 1969.
(58) (a) Hammond, G. S. *J. Am. Chem. Soc.* **1955**, *77*, 334. (b) Lewis, E. *Techniques of Chemistry Volume VI*, 3rd ed.; John Wiley & Sons: New York, 1973.
(59) (a) Conformations of molecules were minimized in energy using Dreiding 2.21 Force Field. Ab initio calculations were performed on minimized structures with MOPAC6 using AM1 Hamiltonian and geometry optimization with Cerius^2 version 1.6 molecular mechanics software. The calculated enthalpies represent the standard enthalpies of reaction. Note that in reaction H, $NaBH_3$-CN was used instead of $LiAlH_4$ in the enthalpy of reaction calculation, due to the fact that MOPAC6 and AM1 are not able to accommodate Li-containing molecules. We note that although the absolute magnitudes of the enthalpies calculated with this method may not be correct, especially for reactions conducted in aqueous media, it is important to emphasize that only the relative trends in the enthalpies with respect to exothermicity are significant for the purpose of evaluating the merit of the Hammond postulate in predicting the plausability of conducting a particular reaction on an imprinted material. (b) Mayo, S. L.; Olafson, B. D.; Goddard III, W. A. *J. Phys. Chem.* **1990**, *94*, 8897.
(60) Hilvert, D. *Curr. Op. Struct. Biol.* **1994**, *4*, 612.
(61) Hsieh, L. C.; Yonkovich, S.; Kochersperger, L.; Schultz, P. G. *Science* **1993**, *260*, 337.
(62) Leonhardt, A.; Mosbach, K. *React. Polym.* **1987**, *6*, 286.
(63) Robinson, D.; Mosbach, K. *J. Chem. Soc., Chem. Commun.* **1989**, 969.
(64) Ohkubo, K.;Urata, Y.; Hirota, S.; Honda, Y.; Fujishita, Y.; Sagawa, T. *J. Mol. Catal.* **1994**, *93*, 189.
(65) Ohkubo, K.; Urata, Y.; Hirota, S.; Honda, Y.; Sagawa, T. *J. Mol. Catal.* **1994**, *87*, L21.
(66) Andersson, L. I.; Mosbach, K. *Makromol. Chem. Rapid Commun.* **1989**, *10*, 491.
(67) Motomura, T.; Inoue, K.; Kobayashi, K.; Aoyama, Y. *Tetrahedron Lett.* **1991**, 32, 4757.
(68) (a) Ohkubo, K.; Urata, Y.; Hirota, S.; Funakoshi, Y.; Sagawa, T.; Usui, S.; Yoshinaga, K. *J. Mol. Catal. A* **1995**, *101*, L111. (b) Reference 68a reports the difference in the activation free energies between the most catalytically active polymer (TP1′) and the uncatalyzed reaction (none) to be 6.4 kcal/mol. This corresponds to a relative rate increase of more than 41 300 for TP1′ over none at 303 K, which is significantly larger than the reported experimentally measured value of 3.7.
(69) Müller, R.; Andersson, L. I.; Mosbach, K. *Makromol. Chem. Rapid Commun.* **1993**, *14*, 637.
(70) Beach, J. V.; Shea, K. J. *J. Am. Chem. Soc.* **1994**, *116*, 379.
(71) Shokat, K. M.; Leumann, C. J.; Sugasawara, R.; Schultz, P. G. *Nature* **1989**, *338*, 269.
(72) Damen, J.; Neckers, D. C. *J. Am. Chem. Soc.* **1980**, *102*, 3265.
(73) Wulff, G.; Vietmeier, J. *Makromol. Chem.* **1989**, *190*, 1727.
(74) Byström, S.; Börje, A.; Akermark, B. *J. Am. Chem. Soc.* **1993**, *115*, 2081.
(75) Sellergren, B.; Shea, K. J. *Tetrahedron A* **1994**, *8*, 1403.
(76) Martin, M. T.; Angeles, T. S.; Sugasawara, R.; Aman, N.; Napper, A. D.; Darsley, M. J.; Sanchez, R. I.; Booth, P.; Titmas, R. C. *J. Am. Chem. Soc.* **1994**, *116*, 6508.
(77) (a) Shea, K. J.; Thompson, E. A. *J. Org. Chem.* **1978**, *43*, 4253. (b) Shea, K. J.; Thompson, E. A.; Pandey, S. D.; Beauchamp, P. S. *J. Am. Chem. Soc.* **1980**, *102*, 3149.
(78) Mathew, J.; Buchart, O. *Bioconjugate Chem.* **1995**, *6*, 524.
(79) Schwanghart, A.-D.; Backmann, W.; Blasche, G. *Chem. Ber.* **1977**, *110*, 778.
(80) Andersson, L. I.; Sellergren, B.; Mosbach, K. *Tetrahedron Lett.* **1984**, *25*, 5211.
(81) Morihara, K.; Kurihara, S.; Suzuki, J. *Bull. Chem. Soc. Jpn.* **1988**, *61*, 3991.
(82) (a) Morihara, K.; Nishihata, E.; Kojima, M.; Miyake, S. *Bull. Chem. Soc. Jpn.* **1988**, *61*, 3999. (b) Morihara, K.; Tanako, E.; Takeuguchi, Y.; Miyazaki, K.; Yamamoto, N.; Sagawa Y.; Kawamoto, E.; Shimada, T. *Bull. Chem. Soc. Jpn.* **1989**, *62*, 499.
(83) Shimada, T.; Kiyoko, N.; Morihara, K. *Bull. Chem. Soc. Jpn.* **1992**, *65*, 954.
(84) (a) Morihara, K.; Doi, S.; Takiguchi, M.; Shimada, T. *Bull. Chem. Soc. Jpn.* **1993**, *66*, 2977. (b) Morihara, K.; Iijima, T.; Usui, H.; Shimada, T. *Bull. Chem. Soc. Jpn.* **1993**, *66*, 3047. (c) Morihara, K.; Nishihata, E.; Kojima, M.; Miyake, S. *Bull. Chem. Soc. Jpn.* **1993**, *66*, 906.
(85) Shimada, T.; Kurazono, R.; Morihara, K. *Bull. Chem. Soc. Jpn.* **1993**, *66*, 836.
(86) (a) Matsuishi, T.; Shimada, T.; Morihara, K. *Bull. Chem. Soc. Jpn.* **1994**, *67*, 748. (b) Morihara, K.; Takiguchi, M.; Shimada, T. *Bull. Chem. Soc. Jpn.* **1994**, *67*, 1078. (c) Shimada, T.; Horose, R.; Morihara, K. *Bull. Chem. Soc. Jpn.* **1994**, *67*, 227.
(87) Morihara, K.; Kurokawa, M.; Kamata, Y.; Shimada, T. *J. Chem. Soc., Chem. Commun.* **1992**, 358.
(88) Bernhard, S.; Gutfreund, H. *Proceedings of the International Symposium on Enzyme Chemistry*, Tokyo and Kyoto, 1957.
(89) Hamilton, C. L.; Niemann, C.; Hammond, G. S. *Proc. Natl. Acad. Sci. U.S.A.* **1966**, *55*, 664.
(90) Heilmann, J.; Maier, W. F. *Angew. Chem., Int. Ed. Engl.* **1994**, *33*, 471.
(91) Ahmad, W. R.; Davis, M. E. *Catal. Lett.*, in press.
(92) Napper, A. D.; Benkovic, S. J.; Tramontano, A.; Lerner, R. A. *Science* **1987**, *23*, 1041.
(93) Heilmann, J.; Maier, W. F. *Z. Naturforsch. B* **1995**, *50*, 460.
(94) Davis, M. E. *Ind. Eng. Chem. Res.* **1991**, *30*, 1675.
(95) Venuto, P. B. *Microporous Mater.* **1994**, *2*, 297.
(96) Davis, M. E.; Lobo, R. F. *Chem. Mater.* **1992**, *4*, 756.
(97) Davis, M. E. *Acc. Chem. Res.* **1993**, *26*, 111.
(98) Csicsery, S. M. *Zeolites* **1984**, *4*, 202.
(99) Weisz, P. B.; Frilette, V. J.; Maatman, R. W.; Mower, E. B. *J. Catal.* **1962**, *1*, 307.
(100) Anderson, M. W.; Klinowski, J. *Nature* **1989**, *339*, 220.
(101) Kucherov, A. V.; Slinkin, A. A.; Gitis, K. M.; Isagulants, G. V. *Catal. Lett.* **1988**, *1*, 311.
(102) Khouw, C. B.; Davis, M. E. *ACS Symp. Ser.* **1993**, *517*, 206.
(103) Perego, G.; Bellussi, C.; Corno, C. Taramasso, M.; Buonomo, F. *Stud. Sur. Sci. Catal.* **1986**, *28*, 129.
(104) Notari, B. *Stud. Sur. Sci. Catal.* **1988**, *37*, 413.
(105) Khouw, C. B.; Dartt, C. B.; Labinger, J. A.; M. E. Davis *J. Catal.* **1994**, *149*, 195.
(106) Li, H. X.; Annen, M. J.; Chen, C. Y.; Arhancet, J. P.; Davis, M. E. *J. Mater. Chem.* **1991**, *1*, 79.
(107) (a) Burkett, S. L.; Davis, M. E. *J. Phys. Chem.* **1994**, *98*, 4647. (b) Burkett, S. L.; Davis, M. E. *Chem. Mater.* **1995**, *7*, 920. (c) Burkett, S. L.; Davis, M. E. *Chem. Mater.* **1995**, *7*, 1453.
(108) Helmkamp, M. M.; Davis, M. E. *Annu. Rev. Mater. Sci.* **1995**, *25*, 161.
(109) Gies, H.; Marler, B. *Zeolites* **1992**, *12*, 42.
(110) (a) Iton, L. E.; Trouw, F.; Brun, T. O.; Epperson, J. E.; White, J. W.; Henderson, S. J. *Langmuir* **1992**, *8*, 1045. (b) Dokter, W. H.; van Garderen, H. F.; Beelen, T. P. M.; van Santen, R. A.; Bras, W. *Angew. Chem., Int. Ed. Engl.* **1995**, *34*, 73.
(111) Regev, O.; Cohen, Y.; Kahet, E.; Talmon, Y. *Zeolites* **1994**, *14*, 314.
(112) Davis, M. E. *Stud. Surf. Sci. Catal.* **1995**, *97*, 35.
(113) Lobo, R. F.; Zones, S. I.; Davis, M. E. *J. Inclus. Phenom.* **1995**, *47*, 21.
(114) (a) Zones, S. I.; Olmstead, M. N.; Santilli, D. S. *J. Am. Chem. Soc.* **1992**, *164*, 4195. (b) Lobo, R. F.; Pan, M.; Chan, I.; Medrud, R. C.; Zones, S. I.; Crozier, P. A.; Davis, M. E. *J. Phys. Chem.* **1994**, *98*, 12040.
(115) Schmitt, K. O.; Kennedy, G. J. *Zeolites* **1994**, *14*, 635.
(116) Li, H. X.; Camblor, M. A.; Davis, M. E. *Microporous Mater.* **1994**, *3*, 117.

CM960019U